CHEMISTRY OF MATERIALS

pubs.acs.org/cm

Perspective

Doped State Engineering in Conjugated Polymers

This Perspective is part of the Chemistry of Materials "Up-and-Coming" series.

Chengwen Wu, Zhi Zhang,* and Ting Lei*

Cite This: *Chem. Mater.* 2026, 38, 3−19

Read Online

ACCESS | Metrics & More | Article Recommendations

ABSTRACT: Doping has long been a central strategy for modulating the performance of organic semiconductors, yet traditional views focusing mainly on carrier density and conductivity are no longer sufficient to account for the complexity of heavily doped systems. Conjugated polymers (CPs), now widely employed in organic thermoelectrics (OTEs) and organic electrochemical transistors (OECTs), exhibit rich electronic and structural transformations upon chemical and electrochemical doping. These doped states critically govern device performance but remain only partially understood. In this Perspective, we provide a detailed explanation of the concept, *doped state engineering*, in CPs, which emphasizes deliberate control over the charge-transfer processes, structural reorganization, and counterion-CP interactions that accompany doping. We highlight how this framework guides advances in molecular design, doping strategies, and processing methods, and we discuss its potential to accelerate the development of high-performance organic electronic materials and devices.

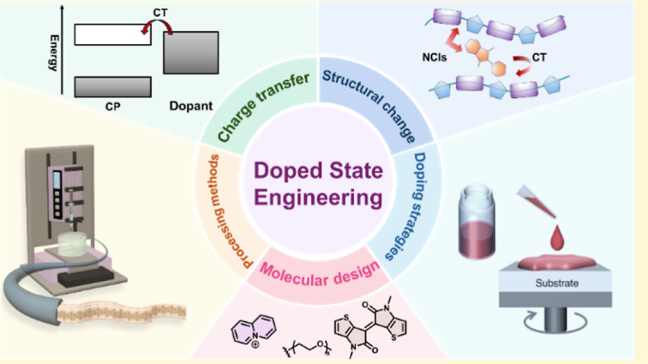

1. INTRODUCTION

Unlike rigid inorganic semiconductors, conjugated polymers (CPs) have emerged as a versatile class of organic semiconductors distinguished by their mechanical softness, stretchability, solution processability, and biocompatibility.[1,2] A critical breakthrough came in the 1970s with the discovery that doped polyacetylene could exhibit remarkably high electrical conductivity, making it the first conductive polymer and ultimately earning the 2000 Nobel Prize in Chemistry.[3] This discovery demonstrates that organic materials under doped states could rival traditional inorganic semiconductors, ultimately inspiring the field of organic electronics.

CPs have already found wide applications, such as in organic photovoltaics (OPVs),[4−6] organic field-effect transistors (OFETs),[7−9] and organic light-emitting diodes (OLEDs).[10,11] These platforms mostly operate in lightly doped regimes, where carriers are field-induced near interfaces and the overall doping fraction remains low (Figure 1a). By contrast, organic thermoelectrics (OTEs) and organic electrochemical transistors (OECTs) represent heavily doped systems (Figure 1b).[9,12,13] In these devices, bulk doping introduces carrier densities usually over 10^{18} cm^{-3}, sometimes approaching 10^{21} cm^{-3}. Unlike inorganic semiconductors, where doping is typically achieved by atomic substitution, doping in organic semiconductors often occurs through charge transfer (CT) between external species and the host system.[14,15] In the former, the dopant atoms are usually covalently bonded to the host atoms (Figure 1c), whereas in organic semiconductors, the charged species generated upon doping are associated with counterions through weak noncovalent interactions (NCIs), such as van der Waals (vdW) interactions (Figure 1d). In addition, unlike inorganic semiconductors where electrons move nearly freely in the bands with little influence from lattice vibrations, organic semiconductors are strong electron−phonon coupling systems. Charge carrier transport is largely limited by hopping between polymer chains,[16] so their distribution along molecular backbones and throughout the system has a significant impact on charge transport properties. These distinctions make organic semiconductor systems more complex.

Heavily doped systems can be further divided into chemical doping and electrochemical doping (Figure 1b). In chemical doping, carriers are introduced usually by small-molecule dopants, which can be mixed with the CPs through solution processing or vapor infiltration, forming bulk-doped systems.[14] In electrochemical doping, the device often operates in aqueous electrolytes or ionic liquids, and the carriers are

Received: September 29, 2025
Revised: December 18, 2025
Accepted: December 22, 2025
Published: December 26, 2025

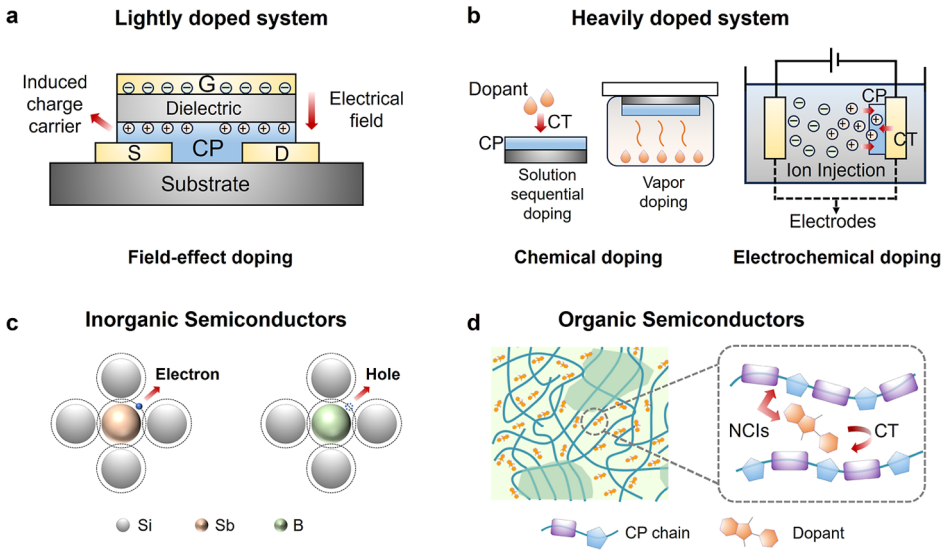

Figure 1. Comparison between lightly and heavily doped systems, and between doping in inorganic and organic semiconductors. (a) Lightly doped (field-effect doping) and (b) heavily doped (chemical and electrochemical doping) systems (taking n-type CP as an example). Reproduced with permission from ref 29 Copyright 2021 John Wiley and Sons. Doping in (c) inorganic semiconductors and (d) organic semiconductors. CT: charge transfer; NCI: noncovalent interaction.

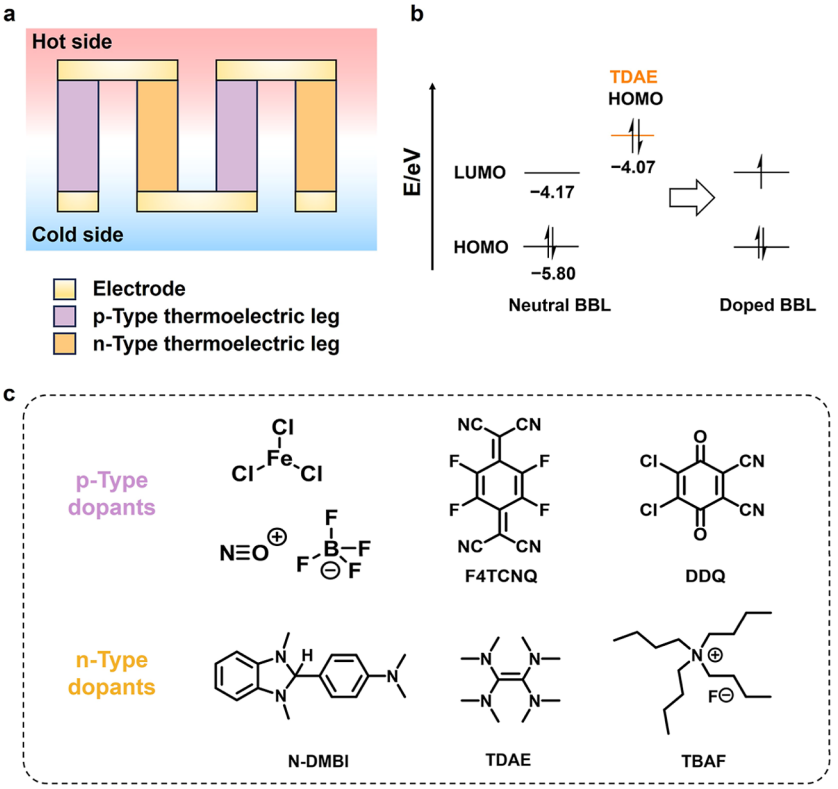

Figure 2. Schematic illustration of a thermoelectric module, chemical doping process, and various dopants. (a) Schematic illustration of a thermoelectric module, where polymers generate a potential difference in the thermoelectric legs driven by a temperature gradient. (b) Schematic illustration of the n-doping reaction electron transfer process (taking BBL and TDAE as an example). (c) Representative p-type and n-type dopants.

introduced via electrochemical redox reactions at the semiconductor−electrode interface, accompanied by the ingress of counterions from the electrolyte into the bulk of the material to maintain charge neutrality.[17] Although chemical and electrochemical doping differ in mechanism and operating environment, both involve bulk charge transfer and high carrier concentrations, making doping efficiency and stability key determinants of performance.

OTEs, relying on chemical doping, convert heat into electricity and offer lightweight, flexible solutions for wearable energy harvesters and self-powered electronics.[12,18,19] OECTs, first demonstrated with polypyrrole in 1984,[20] exploit electrochemical doping to transduce ionic into electronic signals in

https://doi.org/10.1021/acs.chemmater.5c02592
Chem. Mater. 2026, 38, 3−19

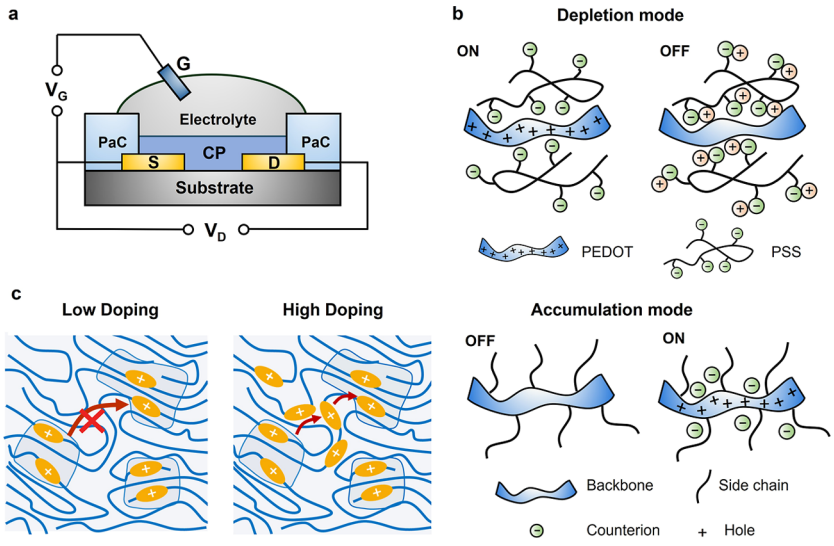

Figure 3. OECT device and mechanism of electrochemical doping. (a) Schematic illustration of an OECT device. (b) Diagrams of polymer doping and switching between depletion and accumulation mode (redrawn according to ref 17). (c) Schematic illustration of the change in p-type polymer charge transport properties during the transition from low doping to high doping (redrawn according to ref 39). When the OECT initially turns on, the low doping level confines holes to the ordered domains (the circled regions), thereby limiting charge transport. Upon reaching higher doping levels, holes extend into the disordered regions, enhancing conduction.

aqueous environments, enabling applications in biosensing, neural interfacing, and neuromorphic devices.[17,21−24] Yet, significant challenges remain. In OTEs, low doping efficiency hampers electrical conductivity (σ) and power factor (PF), while in OECTs, limited electrochemical doping reduces the figure of merit (μC^*) and device stability. These limitations are especially severe for n-type polymers, where doped states often suffer from poor efficiency and instability under oxygen and moisture.

Addressing these challenges requires going beyond conventional views of doping as merely controlling carrier density. More and more research has started to focus on the doped states of CPs, rather than concentrating predominantly on their neutral states as traditionally emphasized.[25−28] In this work, we provide a detailed explanation of the concept of *doped state engineering*: a framework that connects charge-transfer processes with molecular and condensed-state structural changes, and leverages this understanding to guide molecular design, doping strategies, and processing methods. This perspective highlights how doped state engineering can unlock the full potential of CPs in heavily doped applications such as OTEs and OECTs.

2. CHEMICAL DOPING AND ELECTROCHEMICAL DOPING

2.1. Fundamentals of the Thermoelectric Effect and Chemical Doping. Thermoelectric devices can convert a temperature gradient between hot and cold sides into electrical power, and conversely, provide solid-state cooling when an electrical current is applied (Figure 2a). The thermoelectric effect arises from the nonuniform distribution of electrons at the Fermi level, and such asymmetry depends on the shape of the density of states (DOS) function $N(E)$.[30] Doping adjusts the carrier concentration, which also affects the Fermi level, thereby directly influencing two key parameters of thermoelectric materials—σ and the Seebeck coefficient (S). These, in turn, determine the thermoelectric performance metrics—power factor (PF) and figure of merit (ZT)[12]

$$\mathrm{PF} = S^2\sigma \tag{2.1}$$

$$ZT = \frac{S^2\sigma T}{\kappa} \tag{2.2}$$

Therefore, to enhance the performance of thermoelectric materials, it is necessary to increase σ and S, while reducing thermal conductivity (κ). As noted above, doping can modulate carrier concentration, thereby improving σ ($\sigma = nq\mu$, where n is the carrier concentration, q is the elementary charge, and μ is the carrier mobility). However, higher carrier concentration may simultaneously increase κ and reduce S, resulting in a decrease in PF.

For typical organic semiconductors, S can be approximated by eq 2.3,[31] where E_{Tr} is the transport energy level of the polymer, generally located near the center of the DOS distribution (assuming a Gaussian DOS),[32] E_{F} is the Fermi level. For both p-type and n-type semiconductors, doping shifts the Fermi level closer to the transport energy level, leading to a reduction in S. Consequently, achieving the maximum PF usually requires balancing σ and S to identify the optimal doping concentration.

$$S = -\frac{E_{\mathrm{Tr}} - E_{\mathrm{F}}}{qT} \tag{2.3}$$

In essence, chemical doping is a redox process involving electron transfer between the dopant and the polymer (Figure 2b). A typical process is that dopants and polymers react to form doped polymers and counterions. The Gibbs free energy change of this reaction determines the extent to which the doping reaction proceeds, and a more stable doped state could lead to more effective doping. The doping process involves electron transfer between the frontier orbitals of CPs and dopants (Figure 2b, taking poly(benzimidazobenzophenanthroline) (BBL) and tetrakis(dimethylamino)ethylene, (TDAE) as an example).[33] Representative p-type and n-type dopants are shown in Figure 2c. p-Type dopants are mainly oxidants (like Fe^{3+}, NO^+ species, or

https://doi.org/10.1021/acs.chemmater.5c02592
Chem. Mater. 2026, 38, 3−19

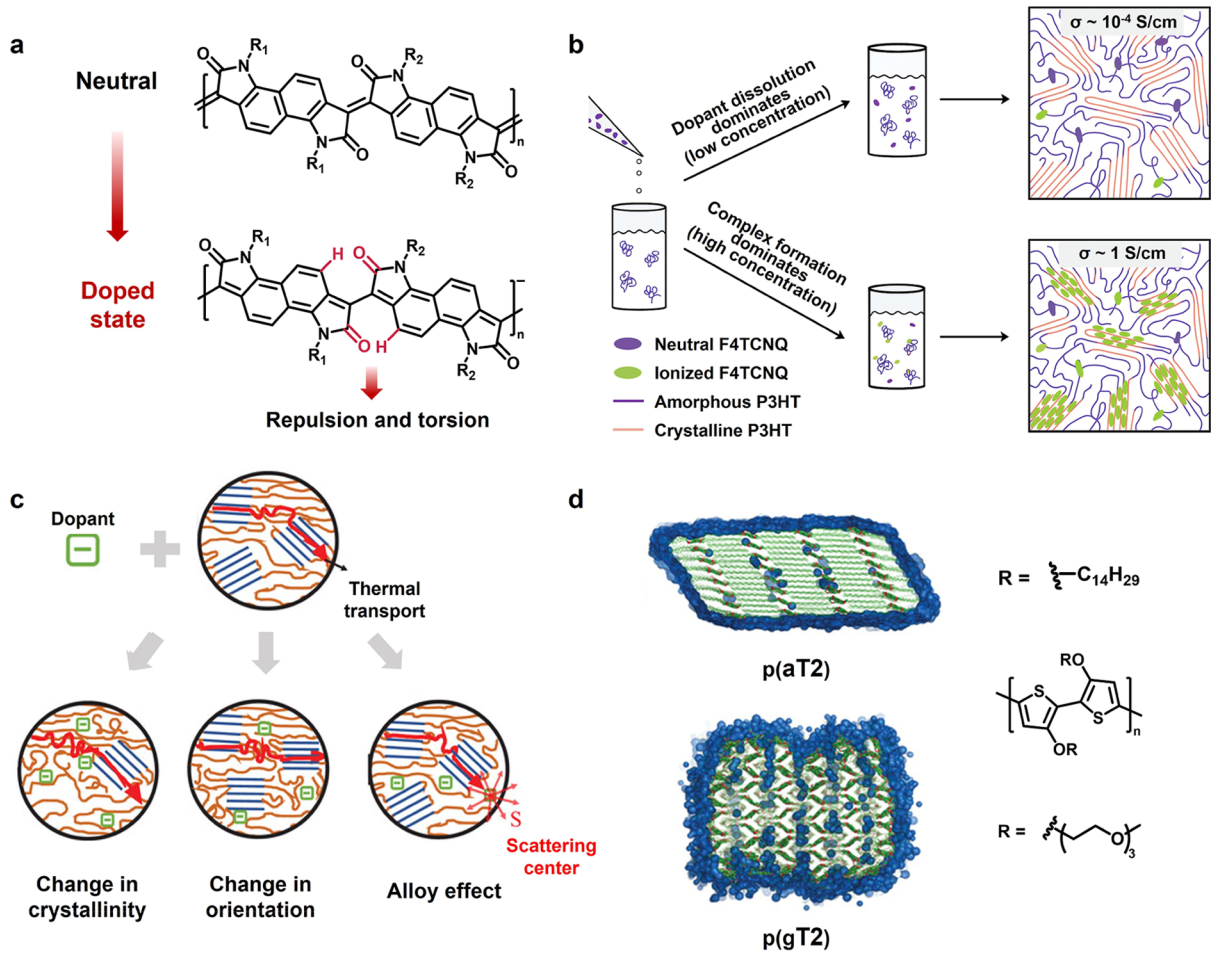

Figure 4. Structure and morphology changes after doping in CP systems. (a) Proposed structural changes (double bond to single bond linkage) in the backbone from the neutral to the doped state, showing that the planar backbone in the neutral state may undergo torsion upon doping. (b) Morphology and conductivity changes of P3HT films at different doping levels. Reproduced with permission from ref 28 Copyright 2021 John Wiley and Sons. (c) Three potential microstructural changes induced by doping of semiconducting polymers. Reproduced with permission from ref 42 Copyright 2025, The Author(s) under the terms of the Creative Commons CC BY license. (d) Schematic of molecular packing changes in OMIECs before and after water absorption. Green: CP chains; blue: water molecules. Reproduced with permission from ref 43 Copyright 2022, The Author(s) under the terms of the Creative Commons CC BY license.

quinone-based compounds with abundant electron-withdrawing groups). n-Type doping mechanisms, by contrast, may involve direct electron transfer to the semiconductor (like TDAE), hydride transfer processes (like (4-(1,3-dimethyl-2,3-dihydro-1*H*-benzoimidazol-2-yl)phenyl)dimethylamine, *N*-DMBI) or nucleophilic attack by anions (like tetrabutylammonium fluoride, TBAF).[18] Notably, for conducting polymers, dopants are incorporated during synthesis, such as poly(3,4-ethylenedioxythiophene)-poly(styrenesulfonate) (PEDOT:PSS) or poly(3,4-ethylenedioxythiophene)-tosylate (PEDOT:Tos), establishing an intrinsically heavily doped state. Post-treatments can then act as dedoping steps by reducing the charge carrier concentrations rather than introducing new ones. For example, PEDOT:Tos can be dedoped through TDAE vapor treatment, which decreases σ while increasing S, resulting in a substantial enhancement in PF (from 38 μW m^{-1} K^{-2} to 324 μW m^{-1} K^{-2}).[34] In this scenario, TDAE functions as a dedoping agent that tunes the carrier concentration to achieve a more favorable balance between S and σ.

The choice of dopant depends on the specific system. Factors such as the highest occupied molecular orbital (HOMO)/the lowest unoccupied molecular orbital (LUMO) energy levels of the dopant and polymer and the intermolecular interactions between them, and the interactions between counterions and polymers after doping can all significantly influence the electron-transfer process, dopant distributions in the polymer matrix, and the charge transport properties of the polymer. Generally, the more readily a dopant donates electrons and the better its miscibility within the host system, the lower and more stable the energy of the doped polymer will be, and consequently the more effective the doping outcome.[35,36]

2.2. OECT and Electrochemical Doping. OECTs are three-terminal devices with a gate (G), a source (S), and a drain (D) electrodes (Figure 3a).[17] Organic mixed ionic–electronic conductors (OMIECs) are commonly employed as the channel materials, bridging the source and drain electrodes while being connected to the gate via an electrolyte. During operation, a drain voltage (V_{DS}) is applied to generate a source–drain current (I_{DS}), which is modulated by the gate voltage (V_{GS}). All voltages are referenced to the grounded source electrode. When a gate voltage is applied, ions in the electrolyte are driven by the electric field into the channel, thereby modifying its doping level and conductivity and

https://doi.org/10.1021/acs.chemmater.5c02592
Chem. Mater. 2026, 38, 3−19

regulating the channel current. Depending on the response of I_{DS} to V_{DS}, OECTs operate in two distinct modes: depletion mode (taking p-type semiconductors as an example, similarly hereafter. I_{DS} decreases with increasing V_{GS}, corresponding to dedoping, from "ON" to "OFF") and enhancement mode (I_{DS} increases with increasing V_{GS}, corresponding to doping, from "OFF" to "ON") (Figure 3b).[17]

The core functionality of an OECT is to transduce weak gate voltage signals into pronounced changes in the drain current. This property is characterized by the transfer curve (the dependence of I_{DS} on V_{GS}). The signal amplification capability is quantified by the transconductance, $g_m = \partial I_{DS}/\partial V_{GS}$, which serves as a key performance metric for transistors. Owing to the bulk doping mechanism, OECTs can achieve exceptionally high transconductance values, where even minor variations in gate voltage induce large current changes. According to the Bernards model,[37] the transconductance can be expressed as

$$g_m = \frac{Wd}{L} \times \mu C^* \times (V_{Th} - V_{GS}) \tag{2.4}$$

where W, L, and d denote the width, length, and thickness of the channel, respectively; μ is the charge-carrier mobility; C^* is the volumetric capacitance; and V_{Th} is the threshold voltage (which reflects the magnitude of the voltage required for the transistor to switch on and off). Since g_m depends on device geometry and biasing conditions, the figure of merit μC^* is typically adopted for an objective evaluation of material performance,[38] which reflects the material's ionic and electronic transport capability.

The fundamental principle of electrochemical doping lies in ion injection into the polymer under a gate bias, resulting in bulk doping that alters the polymer lattice and generates polarons.[40] Unlike field-effect doping in conventional FETs, where no ionic injection occurs, electrochemical doping at low doping levels suffers from reduced μ due to Coulomb traps created by injected ions. At high doping levels, however, μ increases substantially due to Coulomb trap overlapping effects, potentially surpassing that of field-effect systems.[41] In addition to the carrier concentration introduced by doping, the doping rate is also important, as it determines the switching time of the device. In doping kinetics, the doping front may first appear at the polymer−electrode contact and move toward the electrolyte interface. Electrochemical doping speed in CPs is not solely governed by the ion migration rate, but also limited by poor carrier transport at low doping levels, leading to substantially slower switching speeds than expected (Figure 3c).[39] Tuning the molecular structure and packing of CPs helps regulate the efficiency and kinetics of electrochemical doping, thereby modulating the performance of OECT devices.

2.3. Changes in Doped CP Systems. In doped CP systems—particularly in heavily doped systems such as those used in OTE and OECT devices—the materials undergo substantial structure and morphology changes compared with their neutral counterparts. At the molecular level, these changes include the charging of the polymer backbone, the formation of polarons (or bipolarons), and the incorporation of counterions. These processes in turn lead to pronounced alterations in the film morphology as well as in their electrical properties.[28]

For example, in 2021, Sirringhaus et al. reported a series of polymers synthesized from bis-isatin and bis-oxindole monomers.[44] Despite having an electron-deficient backbone and double-bond linkages that suggest good planarity, their FET mobilities were far lower than expected. This was attributed to the fact that, in the doped state, the connecting double bonds convert into single bonds, while torsional strain in the backbone leads to poorer planarity compared with the neutral state (Figure 4a). In other cases, doping can instead enhance the planarity of the polymer backbone. For example, in the OTE material P(Py-2FT), where a higher and steeper torsional barrier of the backbone dihedral angles in the doped state similarly promoted improved molecular packing.[26] In addition, the relative tendency to form polarons versus bipolarons upon doping can strongly affect μ, since bipolaron transport is much less efficient.[45] As a result, material performance can shift dramatically in ways that are not predictable from neutral state molecular design alone. From the morphological perspective, the crystallinity of a polymer can strongly influence its doping level,[46] while doping can conversely alter the polymer's crystalline structure.[47] As illustrated in Figure 4b, increasing the doping level induces the formation of cocrystalline phases composed of dopant−polymer complexes within the film, which in turn leads to a substantial enhancement in electrical conductivity. These findings highlight the need to look beyond pristine systems and focus on the structures and properties of doped molecules, which is particularly critical in heavily doped systems.

For heavily doped systems, the operational characteristics of OTE and OECT devices differ in several important ways. In OTE devices, polymers are typically doped with small-molecule dopants via methods such as solution blending, sequential doping or vapor/solution-phase infiltration. The effectiveness of doping is closely related to doping strategy. For example, in common p-type conjugated polymers bearing alkyl side chains, solution blending often leads to the formation of dopant−polymer complexes that may aggregate, thereby hindering efficient doping and charge transport.[18,48] As a result, p-type doping in such systems is typically carried out via sequential doping or solution/vapor-phase infiltration. In contrast, certain p-type polymers with oligo(ethylene glycol) (OEG) side chains and many n-type polymers can mix well with dopants in solution and are therefore compatible with solution-mixed doping. Beyond its impact on σ, doping can also induce microstructural changes and thereby affect κ. The reduction of κ can arise from altered crystallinity, backbone orientation, or alloy effects (increased scattering centers) (Figure 4c),[42] which is crucial for enhancing the ZT of thermoelectric materials.

In OECT devices, doping/dedoping cycles in an electrolyte allow water molecules to enter the CP film, causing swelling/deswelling and consequently altering morphology.[49] During OECT operation, the swelling of OMIECs can be divided into passive swelling and active swelling.[50] Passive swelling refers to the expansion caused by the intrinsic water uptake of the polymer in the absence of any applied bias. In contrast, active swelling occurs under an applied gate voltage, where ion injection brings accompanying water into the film, leading to additional swelling. When the gate bias is removed, a fraction of the ions and water molecules may remain trapped within the polymer film, which can in turn affect the film morphology. As illustrated in Figure 4d, water can intercalate between polymers and modify their packing. Such structural changes vary with polymer structure. For instance, even within polymers based on the same polythiophene backbone, those bearing OEG side

https://doi.org/10.1021/acs.chemmater.5c02592
Chem. Mater. 2026, 38, 3−19

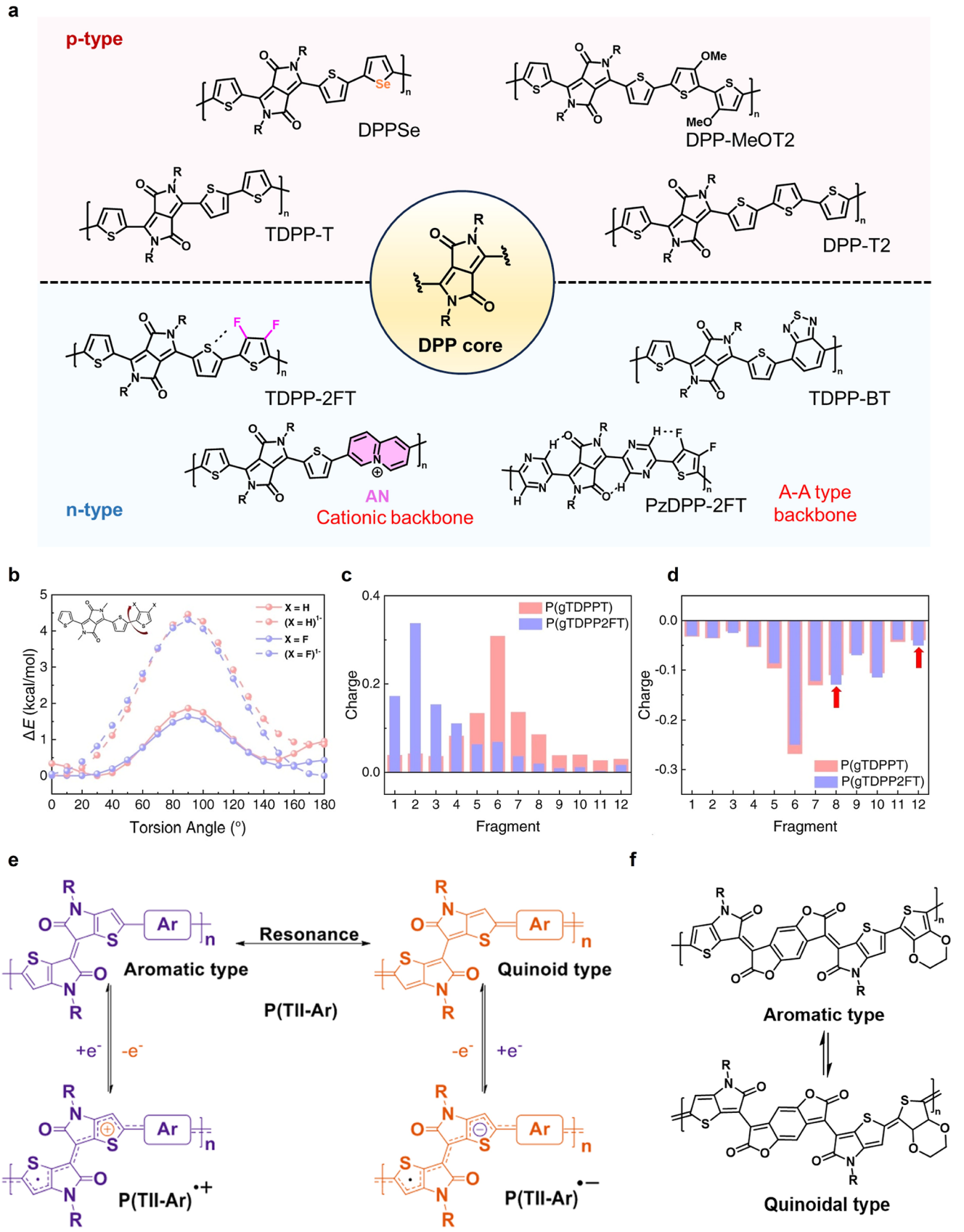

Figure 5. Doped state backbone design in CPs. (a) Starting from a DPP core, a variety of polymer backbones with tunable properties can be designed for both n-type and p-type heavily doped organic semiconductors. (b) Torsional energy barriers of neutral and negatively charged backbones. (c,d) Charge distribution of positively (c) and negatively (d) charged backbones. Reproduced with permission from ref 25 Copyright 2022, The Author(s) under the terms of the Creative Commons CC BY license. (e) Aromatic−quinoidal tautomerization of proquinoidal ambipolar P(TII-Ar) and charge distribution in the doped backbone. Reproduced with permission from ref 58 Copyright 2025 The Author(s)

https://doi.org/10.1021/acs.chemmater.5c02592
Chem. Mater. 2026, 38, 3−19

Figure 5. continued

 (f) Molecular structure of P(TBDOPV-EDOT) and schematic illustration of aromatic−quinoidal tautomerization.

chains tend to adopt a more disordered packing compared with their alkyl side chain counterparts.[43] Recent studies, however, show that although the insertion of water and electrolyte ions increases both lamellar and $\pi-\pi$ stacking distance, the absorbed species do not uniformly permeate the crystallite regions. Instead, they reside in discrete domains. As a result, the overall long-range chain correlations are largely preserved in the hydrated state, providing a mechanistic explanation for why OMIECs can maintain favorable charge transport properties even when swollen with electrolyte.[51]

3. DOPED STATE ENGINEERING IN MOLECULAR DESIGN

3.1. Doped State Backbone Design. Traditional OFET molecular design primarily focuses on optimizing charge injection and charge transport. The former typically tunes the HOMO/LUMO energy levels of individual fragments by introducing electron-donating or electron-withdrawing groups,[52] while the latter mainly focuses on the planarity of the neutral-state backbone[53,54] to achieve better conjugation. Given the significant differences between heavily doped states and neutral states of CPs, the design of polymer backbone cannot rely solely on computational results of the structures optimized for the neutral state. In terms of charge injection, doped state engineering must consider not only the HOMO/LUMO energy levels but also the stability of doped structures, i.e., the Gibbs free energy change (ΔG) associated with the doping process, which depends on many factors, such as the charge distribution along the polymer backbone, backbone structure changes, and counterion interaction with polymers etc. For charge transport, doped state engineering primarily focuses on the planarity of the charged backbone (which is quantified, for example, by torsional statistics such as $\langle\cos^2\varphi\rangle$[53]), torsional barriers, and single dominant planar backbone conformation.[55] Compared with neutral-state backbone design, certain intramolecular interactions—such as hydrogen bonding or S−F interactions—may remain effective, whereas torsional barriers and optimal conformations of the charged backbone can differ substantially from those of the neutral polymer.

Based on these findings, we first proposed the concept of *doped state engineering* while investigating the OECT performance of P(TDPP-2FT).[25] Unlike its analogue P(TDPP-T) (Figure 5a), which exhibited p-type or ambipolar properties, P(TDPP-2FT) showed high n-type OECT performance (μC^* = 54.8 F cm^{-1} V^{-1} s^{-1}). In this example, the doped backbone of P(TDPP-2FT) and P(TDPP-T) reveals a significant increase in torsional barriers, indicating better backbone planarity (Figure 5b). Moreover, different backbones exhibit distinct charge distributions upon doping: P(TDPP-T) maintains relatively uniform charge distributions under both positively and negatively charged states, whereas P(TDPP-2FT) achieves uniformity only under negative charging (Figure 5c,d), explaining why P(TDPP-2FT) lacks ambipolar transport. The introduction of fluorine atoms not only tunes the molecular LUMO level but also stabilizes the backbone through S−F interactions. Additionally, it promotes a more uniform distribution of negative charge along the backbone, enhancing the stability of the doped state. This is the primary reason for the p−n conversion.

Currently, increasing research on CP backbone design is focusing on the doped state. Taking diketopyrrolopyrrole (DPP)-based polymers as an example, tuning the building blocks enables the construction of various p-type and n-type polymers and allows systematic modulation of their electronic properties (Figure 5a). A primary strategy is to adjust the overall energy levels of the molecule. Incorporating electron-rich units into the polymer backbone raises the HOMO level and facilitates p-doping, whereas incorporating electron-deficient units lowers the LUMO level and promotes n-doping. For instance, compared with the DPPS backbone, the DPPSe backbone exhibits a higher HOMO energy (−5.15 eV compared with −5.26 eV) and, upon doping, forms a more ordered molecular packing, which in turn yields improved p-type thermoelectric performance (PF = 364 μW m^{-1} K^{-2}).[56] Conversely, introducing strongly electron-deficient fragments into the backbone—such as the cationic unit 4a-azonianaphthalene (AN) used as an acceptor—yields polymers with extremely low LUMO levels (−4.21 eV) and highly delocalized polarons, leading to high n-type OECT performance (μC^* = 62.3 F cm^{-1} V^{-1} s^{-1}).[57] Moreover, the hydrophilic backbone further facilitates ion injection and diffusion, and the cationic AN can form strong cation−π interactions with DPP core, enhancing the operational stability of OECT devices.

Subsequently, by tuning the relative electron-rich/electron-deficient character of the molecular fragments, one can modulate intramolecular and intermolecular interactions, the degree of polaron delocalization, and the distribution of electronic density along the polymer backbone. At present, most CPs employ donor−acceptor (D−A) type backbones, due to their intrinsic energy offsets between donor and acceptor units, often enable stronger intramolecular charge transfer and have been a research hotspot in molecular design.[59,60] However, studies have shown that excessively large D−A disparities result in strong polaron localization: electrons become confined to acceptor units and holes to donor units, which hampers transport.[61] This also explains why the more electron-rich PDPP-MeOT2 backbone exhibits inferior OECT performance compared with PDPP-T2 (μC^* = 57.5 F cm^{-1} V^{-1} s^{-1} compared with 342 F cm^{-1} V^{-1} s^{-1}). In the design of n-type OTE or OECT materials, increasing efforts also have shifted toward all-acceptor (or acceptor−acceptor, A−A type) designs,[55,62] which help mitigate polaron localization and facilitate doping.

In addition to energy-level tuning, preserving molecular planarity—particularly in the doped state—is also crucial. Representative examples include P(PzDPP-2FT) and P-(TDPP-BT). The former adopts an AA-type backbone and benefits from hydrogen-bonding interactions that promote excellent planarity, enabling improved polaron delocalization and greater disorder tolerance during doping.[55] The latter similarly features a rigid backbone and an increased torsional barrier after doping, which together contribute to its high OECT[63] and OTE[64,65] performance.

For ambipolar molecules, D−A systems usually possess narrower bandgaps, which is favorable for ambipolar transport.

https://doi.org/10.1021/acs.chemmater.5c02592
Chem. Mater. 2026, 38, 3−19

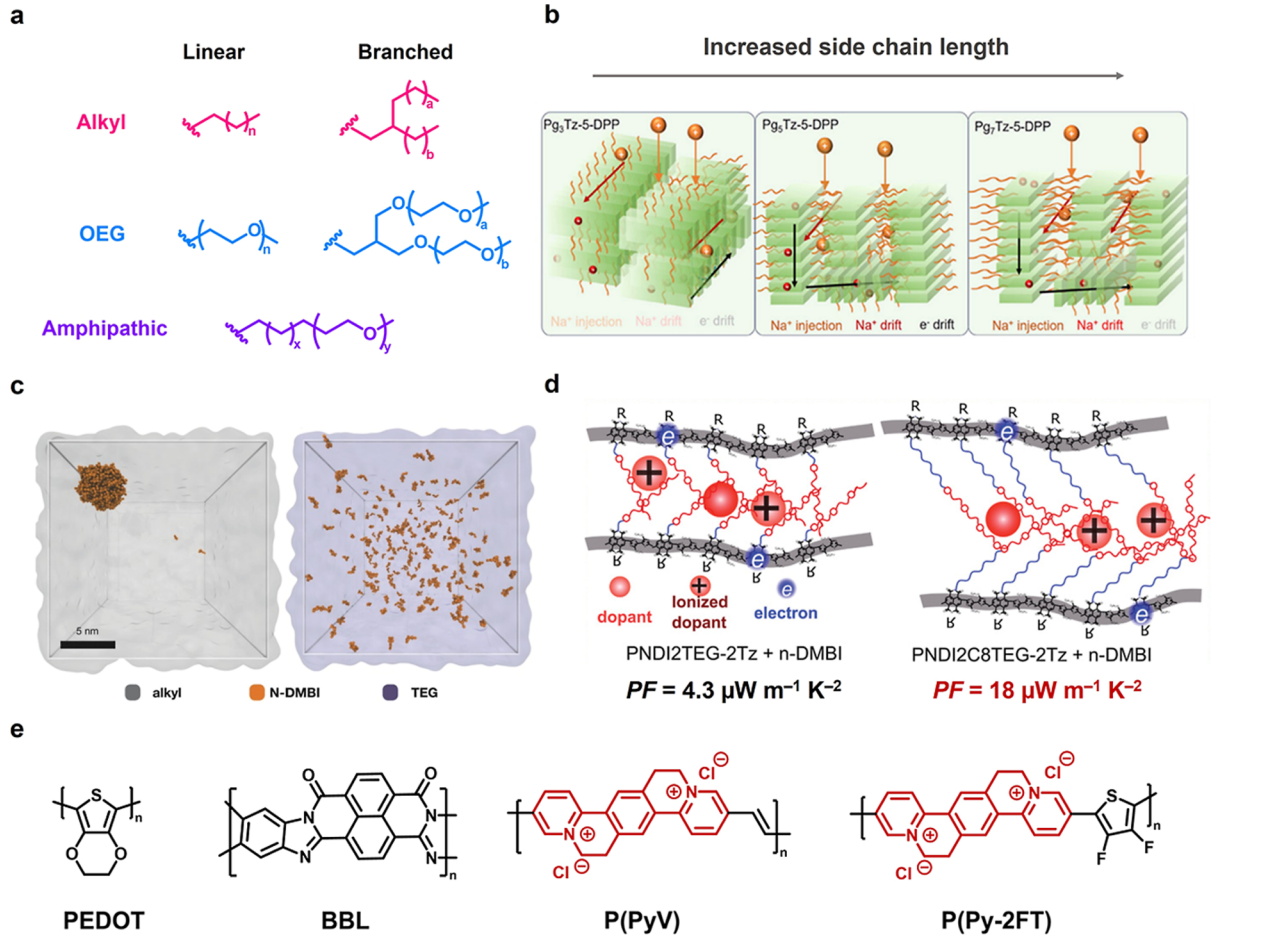

Figure 6. Side-chain engineering in heavily doped CPs. (a) Schematic illustration of several common side chains. (b) Influence of polymer side-chain length on molecular packing, which may further affect electrochemical doping and ion transport. From Pg_3(Tz-5-DPP) to Pg_7(Tz-5-DPP), the length of the OEG side chain increases from 3 to 7 repeat units. Reproduced with permission from ref 73 Copyright 2025 John Wiley and Sons. (c) Representative snapshots from molecular dynamics simulations of *N*-DMBI molecules dissolved in a pure alkyl-N2200 side-chain phase and a pure OEG-N2200 side-chain phase. Reproduced with permission from ref 74 Copyright 2018 John Wiley and Sons. (d) Illustration of the concept of tailoring side chains to control the dopant position relative to the backbone. Reproduced with permission from ref 75 Copyright 2020, The Author(s) under the terms of the Creative Commons CC-BY-NC-ND license. (e) Illustration of several side-chain-free CPs.

Although increasing the donor−acceptor energy offset can lead to narrower bandgap, it often comes at the expense of stronger polaron localization and poor ambipolar OECT performance and stability. To address this, we proposed the design of proquinoidal units.[58,66] Taking thienoisoindigo (TII)-based polymers as an example, their small singlet−triplet energy gap (ΔE_{ST}) facilitates aromatic−quinoid resonance (Figure 5e). The quinoid structure significantly enhances electronic delocalization between segments. Meanwhile, its diradical character enables the system to readily accept or donate electrons, thereby promoting doping. Moreover, the doped states also exhibit good electronic delocalization. These factors enabled the P(TII-2FT) molecule to achieve high and well-balanced ambipolar OECT performance (μC^* of p-type: 158.6 F cm^{-1} V^{-1} s^{-1}; μC^* of n-type: 147.4 F cm^{-1} V^{-1} s^{-1}).[58] Subsequently, we employed a strong proquinoidal acceptor, thiophene-fused benzodifurandione-based oligo(*p*-phenylene-vinylene) (TBDOPV) to further validate the effectiveness of proquinoidal design for ambipolar OECTs (Figure 5f). Polymer P(TBDOPV-EDOT), with a 3,4-ethylenedioxythiophene (EDOT) donor, achieved excellent ambipolar OECT performance (μC^* of p-type: 268 F cm^{-1} V^{-1} s^{-1}; n-type: 107 F cm^{-1} V^{-1} s^{-1}).[66]

In summary, given the clear differences between doped and neutral states, we emphasize the importance of tuning doped state backbone planarity and charge distribution through careful design of copolymer units or their energy-level matching. This highlights the critical significance of doped state backbone design in achieving high-performance organic electronic materials.

3.2. Side-Chain Engineering for Modulating Counterion Interactions. The design of doped state backbones aims to address the distribution of charge carriers within charged polymers, while the design of side chains in the doped state serves to regulate interactions between counterions and the backbone. In conventional CP molecular design strategies, side-chain engineering has primarily focused on tuning solubility and molecular packing,[67] without considering the counterion issue in heavily doped systems. By modulating the polarity and geometric configuration of side chains, the interactions between side chains and counterions can be significantly altered. Currently, CPs' side chains can be classified by polarity into alkyl side chains, OEG side chains, and amphipathic side chains combining both; geometrically, they can be divided into linear and branched chains (Figure 6a).[68] Due to differences in operating environments and

https://doi.org/10.1021/acs.chemmater.5c02592
Chem. Mater. 2026, 38, 3−19

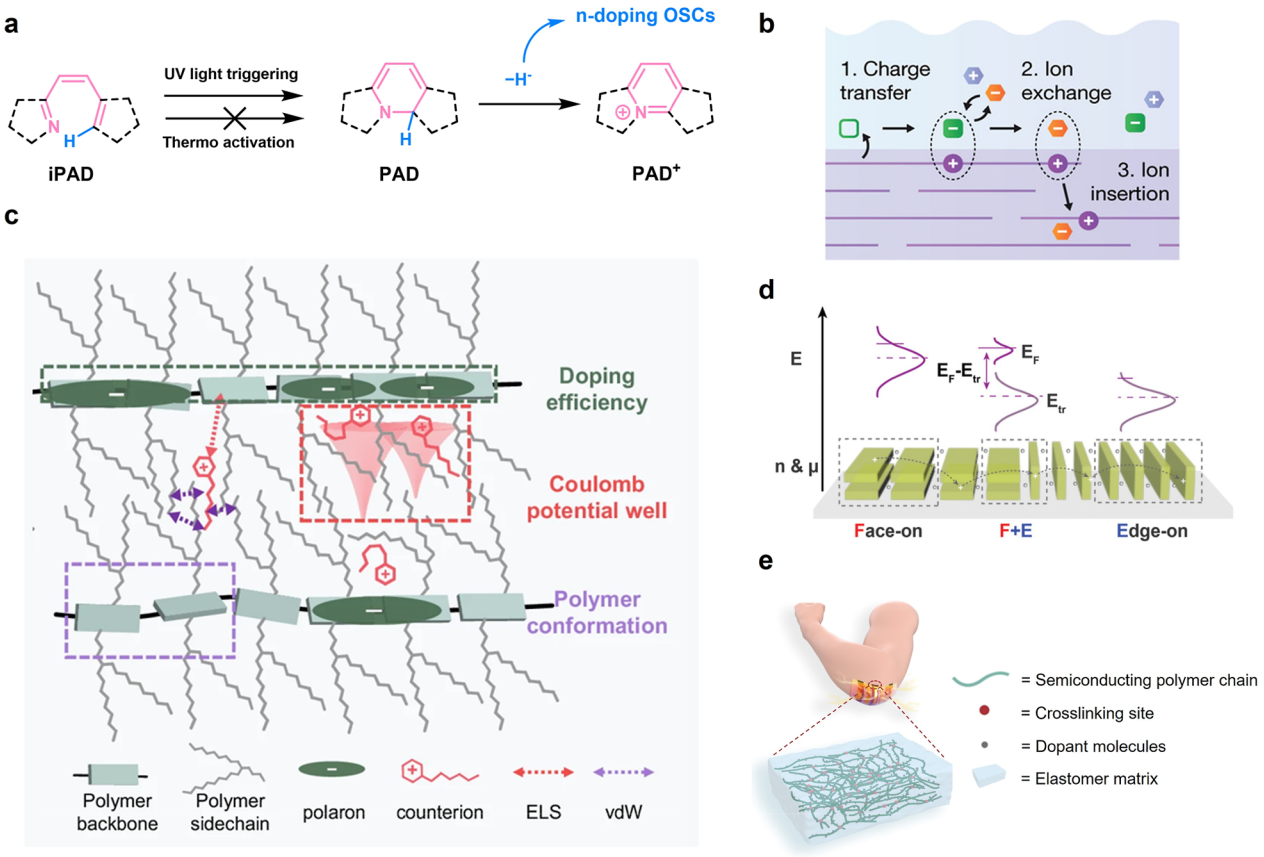

Figure 7. Doping and processing strategies in OTE materials. (a) Schematic illustration of light-triggered n-doping methods (redrawn according to ref 92). (b) Ion-exchange doping mechanism. Reproduced with permission from ref 94 Copyright 2021, The Author(s) under the terms of the Creative Commons CC BY license. (c) Counterion docking affects the doping efficiency, the distribution of Coulomb potential well, and the polymer backbone conformation. Reproduced with permission from ref 95 Copyright 2024, The Author(s) under the terms of the Creative Commons CC BY license. (d) Illustrations of correlation between molecular orientations and TE-related properties. Reproduced with permission from ref 98 Copyright 2022 John Wiley and Sons. (e) Schematic illustration of n-type thermoelectric elastomers. Reproduced with permission from ref 99 Copyright 2025 Springer Nature.

counterions, the effects of side chains on OECT and OTE systems vary. For OECTs, which typically operate in aqueous environments, OEG side chains, owing to their hydrophilicity, interact more strongly with metal ions such as sodium in solution, thereby facilitating ion penetration and often leading to superior performance compared with polymers with alkyl side chains.[69,70] More recently, amphipathic side chains have been explored as alternatives to OEG, balancing ion transport while mitigating the structural disorder induced by strong OEG−backbone interactions.[71] However, for electrochemical doping in ionic liquid environments, polymers with alkyl side chains may instead be advantageous, as the alkyl side chains exhibit stronger interactions with organic ammonium ions.[72] The length of side chains may also play a crucial role. For instance, in polymers Pg_x(Tz-5-DPP) with linear OEG side chains of varying lengths (x = 3 to 7). Variations in side-chain length affect not only molecular packing but also counterion injection and ion−electron transport. It was observed that increasing chain length caused the stacking orientation to gradually shift from edge-on (unfavorable for ion injection) to mixed edge-on/face-on, and eventually to predominantly face-on (unfavorable for electron transport). Optimal OECT performance was achieved at x = 5, where the mixed stacking mode balanced ion and electron transport (Figure 6b).[73]

For OTE materials, traditional designs almost exclusively employed alkyl side chains. Linear and branched chains also show distinct effects: linear chains generally induce more ordered, tighter molecular packing but reduce solubility and processability. Researchers have found that an asymmetric design with a linear chain on one side and a branched chain on the other improves the packing of branched chains and allows dopants to approach the backbone more closely.[76] Compared with alkyl side chains, OEG side chains often favor chemical doping, as their flexible conformations and strong polarity (stronger interaction with dopants) enhance dopant dispersion (Figure 6c).[74] The oxygen atoms in the OEG side chains can coordinate with the cations formed from the n-dopant after doping, thereby stabilizing the system. Amphipathic side chains have also been applied to OTEs; by replacing OEG with amphipathic side chains, the relative location of dopants to the backbone can be controlled, alleviating the negative packing effects of OEG while increasing S without compromising σ (Figure 6d).[75,77] More recent work has focused on refined side-chain modifications, such as fluorination at chain termini, which helps suppress the quenching of doped carriers by oxygen and moisture in air.[78]

In contrast to side-chain-bearing polymers, side-chain-free polymers—lacking the steric separation imposed by substituents—often exhibit stronger dopant ion−backbone interactions and tighter packing, which favor charge transport, offering broad prospects for development. Some representative side-chain-free polymers are shown in Figure 6e. For example,

https://doi.org/10.1021/acs.chemmater.5c02592
Chem. Mater. 2026, 38, 3−19

well-developed systems such as the PEDOT family,[79,80] polypyrrole (PPy),[81] and the ladder-type polymer BBL[82−84] have already found wide application in OECT and OTE devices and can even be processed into fibers for wearable electronics. These polymers could exhibit higher electrical conductivity than side-chain-bearing CPs (reaching up to σ = 4380 S cm^{-1} for PEDOT:PSS[85]). However, their poor solubility often necessitates the introduction of different counterions[86,87] to enable tunable performance. Recently, cationic backbone side-chain-free polymers have also been reported. Such cationic backbones not only enhance doping ability due to their electron-deficient nature but also possess good water solubility and can form physical cross-links with bidentate anions. Based on this principle, our group developed the first n-type semiconducting hydrogel using P(PyV), which achieved both functional semiconductor circuits and favorable biointerfaces.[88] These cationic polymers also show potential in thermoelectrics. For example, P(Py-2FT) exhibits good backbone planarity, and in the doped state its molecular packing becomes denser, endowing the material with a high σ of up to 28.1 S cm^{-1} and a high PF of up to 28.7 μW m^{-1} K^{-2}, comparable to many conventional n-type OTE polymers.[26]

4. DOPED STATE ENGINEERING IN PROCESSING STRATEGIES

4.1. Doping and Processing Strategies in OTE. At the device level, doped state engineering aims to explore the relationship between the three-dimensional condensed-state structure of doped systems and their performance, while also optimizing material processing and device fabrication. For OTEs, the key objectives of doped state engineering contain two parts: (i) to achieve efficient and controllable doping, and (ii) to precisely regulate the morphology of the CP thin film under doping. To realize efficient and controllable doping, one feasible strategy beyond optimizing polymer molecular design is the development of improved dopants. For example, as early as 2017, OEG chains were introduced onto the commonly used dopant *N*-DMBI to enhance compatibility with polymer systems.[89] Another approach involves catalytic/activated doping, where photoactivated[90] and transition-metal-catalyzed doping[91] strategies have been reported. Recently, Pei et al. developed a photocyclization strategy that converts inactive photoactivable dopants (iPADs) into highly reactive photo-activated dopants (PADs), enabling controllable doping with micrometer-level resolution (Figure 7a).[92,93]

In addition to dopant design, ion-exchange doping has emerged as a powerful tool in recent years.[12,94−96] Ion exchange in PEDOT systems was accomplished at an early stage by Rudd et al., who demonstrated that counterion effects markedly affect charge transport in conducting polymers.[97] By selecting appropriate counterions, the stacking of the polymer chains can be tuned, enabling simultaneous optimization of both σ and μ. Chemical doping typically involves the formation of a charge-transfer complex (CTC) between the polymer and the dopant, which eventually yields a charged polymer and a counterion. However, this reaction may be a reversible equilibrium and is not always complete. Ion exchange, by replacing the counterion with a more stable one, can drive the doping reaction forward (Figure 7b).[94] Nevertheless, this introduces new challenges, as different counterions can induce distinct NCIs with the polymer, thereby leading to varying degrees of energetic disorder in the system.[12] We found that three major factors need to be considered: the doping efficiency of different counterions, the distribution of Coulomb potential wells, and the torsional characteristics of the backbone (Figure 7c). Screening studies have revealed that aromatic cations, compared with alkyl cations, tend to induce less energetic disorder and thereby enable more effective doping in some polymers with alkyl side chain.[95]

The precise control of CP thin film morphology remains one of the central challenges in elucidating the structure−property relationship of organic semiconductors. First, it dictates DOS distribution, which characterizes energetic disorder, thereby influencing doping behavior, charge transport, and ultimately properties such as μ, S, and σ.[100,101] The morphology of CPs can be tuned through processing methods: since polymers are typically processed from solution, the choice of processing solvent can strongly influence thin-film morphology. Our previous study demonstrated that in chemical doping system, by tuning the type of processing solvent, temperature, and aging time, the aggregation tendency of polymers in solution can be effectively regulated, which in turn modulates the miscibility of polymers with dopants and the film morphology, thereby enabling considerable control over the electrical conductivity.[102]

For instance, processing FBDPPV-OEG polymer with different solvents (chloroform (CF), hexafluoroisopropanol (HFIP), and ortho-dichlorobenzene (*o*-DCB)) regulates aggregation and thereby the DOS width.[100] In *o*-DCB, the polymer shows the strongest aggregation, resulting in narrow DOS distribution and high μ; however, its low doping efficiency limits its σ. In contrast, HFIP leads to broader DOS distribution and much higher doping efficiency, yielding the highest σ. Treatment with CF produces an intermediate DOS distribution and corresponds to the highest PF. Di et al. further explored controlling polymer packing by solution shearing. By adjusting the ratio of PVDF55:HFP45 to [EMIM][TFSI], they tuned DPP-BTz to adopt either a face-on orientation or a bimodal orientation (mixed edge-on and face-on). Compared with polymers exhibiting a single orientation, those with a bimodal orientation facilitate dopant penetration between chains.[98] In the meantime, aligning E_F and E_{Tr} in distinct regions while achieving increased splitting between E_F and E_{Tr} and enhancing both S and σ (Figure 7d). Besides, structuring CPs into fibrous architectures presents a unique pathway for enhancing thermoelectric performance. We demonstrated that a flow-enhanced crystallization (FLEX) method can continuously produce ultratough and highly aligned semiconducting polymer fibers that combine exceptional mechanical properties (tensile strength >200 MPa, toughness >80 MJ m^{-3}) with strain-enhanced electrical conductivity upon n-doping, yielding a high PF of 146 μW m^{-1} K^{-2}.[103] This work demonstrates how processing-induced alignment and crystallinity control can synergistically optimize mechanical and electronic properties for durable, efficient fiber-based thermoelectrics.

In addition to tuning the electronic properties, the thermal conductivity of OTE materials can also be engineered through morphology control. By blending different CPs or forming composites with other materials, interfacial phonon scattering can be enhanced to reduce κ. In 2024, a polymeric multiheterojunction (PMHJ) strategy was reported, where alternating PDPPSe-12:PBTTT layers yielded over a 60% reduction in κ and exhibited a ZT of 1.28 at 368 K.[104] Recently, our group proposed blending CPs with rubbers and developed the first n-type thermoelectric elastomers: the

https://doi.org/10.1021/acs.chemmater.5c02592
Chem. Mater. 2026, 38, 3−19

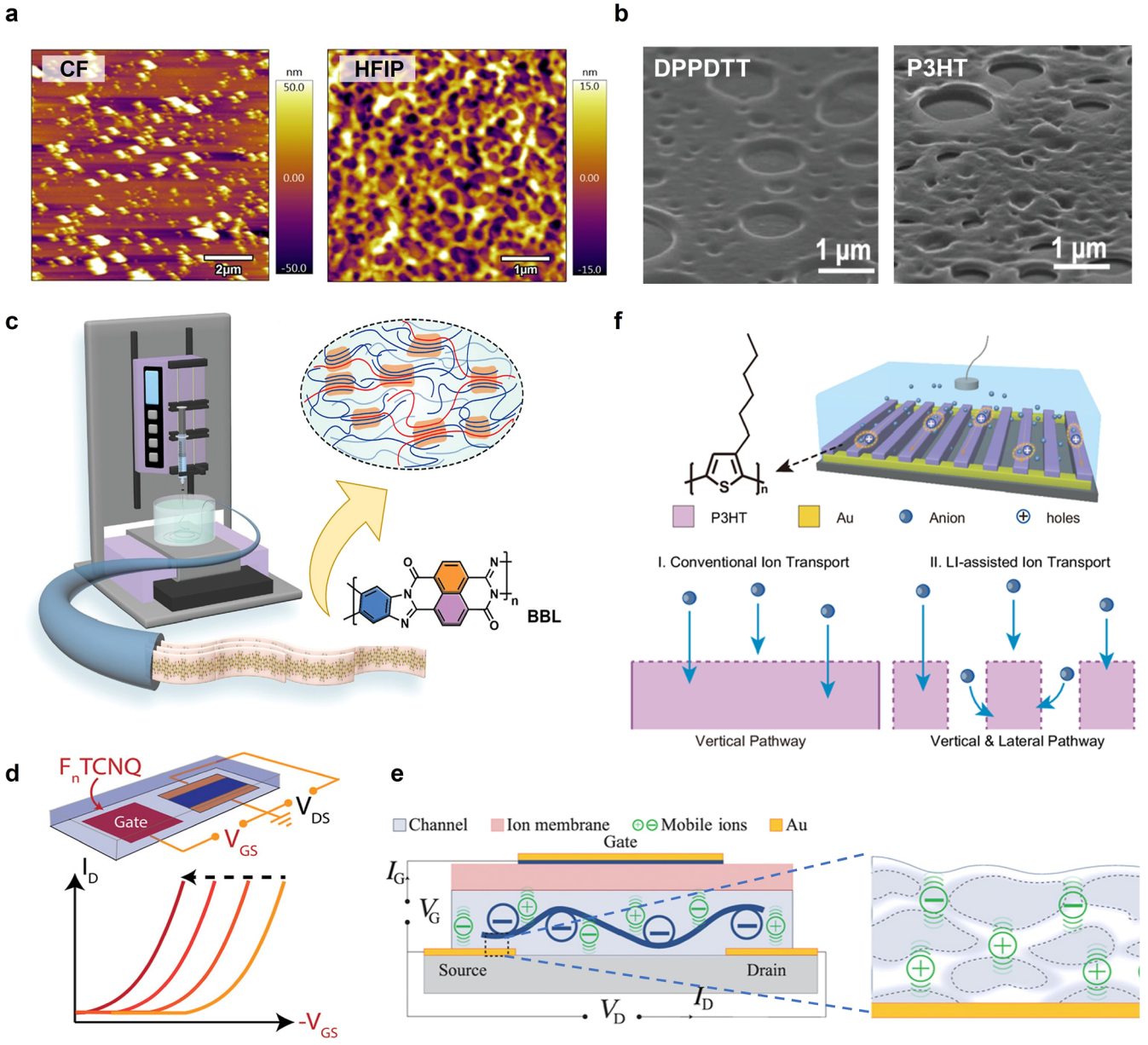

Figure 8. Morphology control and device design in OECT. (a) AFM topography images of the spin-coated P(bgDPP-MeOT2) film using CF (left) and HFIP (right) as solvents. Reprinted with permission from ref 68 Copyright 2021, The Royal Society of Chemistry. (b) Porous film SEM images of p-DPPDTT, p-P3HT. Reprinted with permission from ref 108 Copyright 2021, John Wiley and Sons. (c) Schematic illustration of the fabrication BBL fibers and BBL molecular chain arrangements in fibers. Reprinted with permission from ref 109 Copyright 2024, John Wiley and Sons. (d) Schematic illustration of tuning the transfer curve by adjusting the doping level of the gate OMIEC. Reproduced with permission from ref 110 Copyright 2022, John Wiley and Sons. (e) Schematic illustration of IGT cross-section and wiring diagram for device operation (left). PEDOT:PSS was simultaneously used as the channel material and the gate modification layer (blue). D-Sorbitol creates an ion reservoir, maintaining mobile ions (green) that can travel within the channel; PEDOT-rich regions are shown in light blue and PSS lamellas in white (right). Reproduced with permission from ref 111 Copyright 2019, The Author(s) under the terms of the Creative Commons CC-BY-NC license. (f) Schematic of device configuration and molecular structure of P3HT. I. Conventional ionic transport: ions penetrate into the channel mainly dominated by the vertical pathway. II. LI-assisted ionic transport: ion transports through a synergistic effect of the lateral and vertical pathways. Reproduced with permission from ref 112 Copyright 2024, The Author(s) under the terms of the Creative Commons CC-BY-NC-ND license.

inherently low thermal conductivity of rubbers, combined with enhanced interfacial scattering from blending, reduces overall thermal conductivity (taking Pg_7TDPP-BT as an example, κ decreases from 0.62 W m^{-1} K^{-1} to 0.31 W m^{-1} K^{-1}); meanwhile, dopants preferentially aggregate along CP nanofibrils, improving doping efficiency and conductivity (26.8 S cm^{-1} compared with 22.5 S cm^{-1} for Pg_7TDPP-BT). This strategy not only yields higher ZT values than pristine polymers (0.49 compared with 0.19 for Pg_7TDPP-BT) but also imparts elasticity that is hardly achievable with inorganic thermoelectrics (Figure 7e).[99]

4.2. Morphology Control and Device Design in OECT.

Unlike OTE materials, which emphasize precise control of the Fermi level and DOS distribution, OECT materials focus more on their responsiveness to biological signals under physiological conditions. This requires a high μC^* (to achieve strong signal amplification), a small V_{Th} (for easier switching and lower power consumption), and a fast response speed (to

https://doi.org/10.1021/acs.chemmater.5c02592
Chem. Mater. 2026, 38, 3−19

sensitively capture high-frequency biological signals).[21,23] Performance tuning of OECT can already be effectively achieved through building block design and side-chain engineering. For example, incorporating strong electron-withdrawing groups may increase μC^* and reduce V_{Th},[57] while tuning the length or branching position of OEG side chains allows control over both solubility and ionic permeability.[68,105] For biosignal detection, further improvement and functionalization can be realized through the fabrication of bioelectronic devices composed of multiple OECTs, such as inverters or by optimizing device architectures.[58,106] Moreover, processing strategies that regulate polymer thin-film morphology can also significantly impact doping performance. In general, high-performance and stable OECT devices require film morphologies that satisfy three conditions:[107] (i) relatively close molecular packing and good connectivity between adjacent crystalline domains to achieve high charge carrier mobility. (ii) Sufficient free volume and efficient ionic transport pathways to facilitate ion uptake and transport, and (iii) the ability to suppress microstructural damage caused by ion incorporation, thereby mitigating the detrimental effects of film swelling on charge transport.

Regarding specific processing methods, a common strategy is annealing, where annealed films typically exhibit higher crystallinity and μ, and may also show improved device stability.[113,114] In addition, similar to chemical doping systems, in electrochemical doping systems, morphology can also be tuned by adjusting the solvent. For instance, our group found that when dissolving P(bgTDPP-MeOT2) with HFIP, the GPC-measured molecular weight was significantly lower than that obtained using *o*-DCB or CF, suggesting that polymer aggregation likely occurs in *o*-DCB or CF solutions.[68] Atomic force microscopy (AFM) characterization also revealed distinct differences: films processed from CF contained large aggregates, whereas those from HFIP formed a more uniform network structure (Figure 8a), the latter being more favorable for ion doping and charge transport. Solvents can also be employed for post-treatment. For example, annealing PEDOT:PSS films by soaking in dimethyl sulfoxide (DMSO) enhances structural order and significantly improves carrier mobility and long-term stability.[115] Beyond aggregate morphology control, tuning the surface properties of CPs also benefits OECT performance. Optimization at the polymer−electrolyte interface has been reported. Facchetti et al.[108] spin-coated hydrophobic polymers under humid conditions and then evaporated water and solvent to form porous polymer films (Figure 8b). This structure facilitated ion penetration, enhanced doping, and resulted in high transconductance. Processing CPs into highly aligned fibers presents a distinct strategy to enhance OECT stability and transconductance.[103,109] As demonstrated by wet-spinning the ladder polymer BBL into microfibers, this process induces tight molecular packing and high orientation along the fiber axis (Figure 8c).[109] The resulting robust microstructure significantly suppresses detrimental swelling during electrochemical cycling, enabling n-type fiber OECTs to maintain exceptional operational stability over 1500 cycles, a marked improvement over their thin-film counterparts. This approach highlights the critical role of advanced processing in achieving stable doped states for durable bioelectronics.

In addition to polymer processing, doping optimization can also be accomplished through device engineering. For instance, treatments of the gate electrode can modulate the doping characteristics. Salleo et al. reported replacing the conventional Ag/AgCl gate with an OMIEC gate. By chemically doping the OMIEC gate, V_{GS} could be tuned without altering the conduction properties of the channel, thereby enabling control over V_{Th} and the power consumption (Figure 8d).[110] Device structure optimization can likewise modulate electrochemical doping and OECT response speed, with conventional strategies including the reduction of device dimensions.[116] Recently, the ion-gated organic electrochemical transistor (IGT) was introduced to address this challenge (Figure 8e). In IGTs, the gate is connected to the channel through an ion reservoir (e.g., D-sorbitol), which dramatically reduces the distance of ion migration, thereby accelerating the electrochemical doping process and enabling sensitive detection of high-frequency bioelectrical signals.[111] Moreover, constructing lateral intercalation (LI) facilitates faster lateral ion transport and enhances doping uniformity (Figure 8f), enabling higher g_m and shorter response times.[112]

5. CONCLUSION AND OUTLOOK

From inorganic to organic semiconductors, doping has always been a crucial approach for tuning material properties. *Doped state engineering* focuses on the doping process and the doped state itself, aiming to understand how doping can occur efficiently, controllably, and rapidly, how the doped state can be stabilized, and how structural changes induced by doping correlate with charge transport performance. Benefiting from the rich structural diversity and tunability of CPs, these insights can then guide the molecular design of CPs, the choice of doping strategies, and device-processing methods.

From the perspective of doped state engineering, several factors should be considered when designing polymer for heavily doped systems, like OTE or OECT:

1. Backbone design: It is important to consider the overall HOMO/LUMO levels of the polymer, the energy level alignment between different segments, and the charge distribution along the charged backbone to ensure efficient and stable carrier injection. Attention should also be paid to the planarity of the charged backbone to facilitate efficient carrier transport. These properties can be preliminarily assessed using density functional theory (DFT) calculations.
2. Side-chain and dopant selection: Apart from the oxidative/reductive capability of the dopants, the miscibility and spatial distribution of dopants or counterions and their interactions with the polymer in different side-chain systems should be taken into account. For example, in OECTs, OEG side chains aid water and counterion injection, while in OTEs, OEG side chains stabilize and interact with dopant ions, potentially affecting performance. These factors can also be predicted using DFT and molecular dynamics (MD) simulations.
3. Device fabrication: Polymers may preaggregate in solution, thereby affecting film morphology. For OTEs, selecting suitable solvents and dopants allows morphology control and thus regulation of the DOS distribution and doping efficiency. For OECTs, solvent-related factors must likewise be tuned to maintain morphological stability during doping−dedoping process. Device structure optimization could also affect doping and device stability.

https://doi.org/10.1021/acs.chemmater.5c02592
Chem. Mater. 2026, 38, 3−19

In conclusion, for heavily doped systems, such as OTEs and OECTs, intensive chemical or electrochemical doping induces substantial structural changes, further underscoring the importance of doped state engineering.[117,118] Therefore, this perspective aims to extend current molecular design strategies beyond the neutral state and place greater emphasis on the doped state and its associated structure−property relationships, regardless of whether the material is p-type, n-type, or ambipolar.

At present, in the OTE field, further efforts are needed to precisely regulate the packing of doped state polymers to control DOS, and to elucidate the microscopic mechanisms of carrier transport.[119] In addition, the long-term stability in air as well as the thermal stability of the materials need to be further improved.[78] In the OECT field, key challenges include achieving efficient, rapid, and selective electrochemical doping in the complex environment of biological fluids, maintaining stability during repeated doping−dedoping cycles, and avoiding adverse immune responses in vivo—all of which remain critical considerations for material and device design.[21] Looking forward, doped state engineering will play an increasingly pivotal role in bridging fundamental molecular insights with practical device applications. Future efforts should not only focus on tailoring doped state structures for improved stability and performance, but also on establishing a unified understanding of structure−function relationships across different material systems. Such advances are expected to accelerate the translation of CPs into robust, high-performance wearable electronics and bioelectronics.

AUTHOR INFORMATION

Corresponding Authors

Zhi Zhang − *National Key Laboratory of Advanced Micro and Nano Manufacture Technology, Key Laboratory of Polymer Chemistry and Physics of Ministry of Education, School of Materials Science and Engineering, Peking University, Beijing 100871, P. R. China*; Email: zhizhang@pku.edu.cn

Ting Lei − *National Key Laboratory of Advanced Micro and Nano Manufacture Technology, Key Laboratory of Polymer Chemistry and Physics of Ministry of Education, School of Materials Science and Engineering, Peking University, Beijing 100871, P. R. China*; orcid.org/0000-0001-8190-9483; Email: tinglei@pku.edu.cn

Author

Chengwen Wu − *National Key Laboratory of Advanced Micro and Nano Manufacture Technology, Key Laboratory of Polymer Chemistry and Physics of Ministry of Education, School of Materials Science and Engineering, Peking University, Beijing 100871, P. R. China*

Complete contact information is available at: https://pubs.acs.org/10.1021/acs.chemmater.5c02592

Author Contributions

The manuscript was written through contributions of all authors. All authors have given approval to the final version of the manuscript.

Notes

The authors declare no competing financial interest.

Biographies

Chengwen Wu received his B.S. degree in Chemistry from Peking University in 2025. He joined Lei's group in 2024 and is currently pursuing his Ph.D. degree in Materialogy at Peking University. His research focuses on the molecular design of conjugated polymers and organic thermoelectric materials.

Zhi Zhang received her B.S. from Qingdao University in 2014 and Ph.D. from Donghua University in 2020. From 2021 to 2023, she conducted postdoctoral research with the Lei Ting group at Peking University. She is currently an Associate Researcher at the School of Materials Science and Engineering, Peking University. Her research focuses on the design, development, and applications of organic semiconductor fibers and wearable electronic sensors.

Ting Lei received his B.S. and Ph.D. degrees from Peking University in 2008 and 2013, respectively. After postdoctoral training at Stanford, he joined Peking University in 2018. He is a Boya Distinguished Professor in School of Materials Science and Engineering at Peking University. His current research focuses on organic/polymeric semiconductors and their applications in flexible electronics, bioelectronics, and spintronics.

ACKNOWLEDGMENTS

This work is supported by National Key R&D Program of China (2024YFF0509300), National Natural Science Foundation of China (T2425010 & T2521001). The authors appreciate Suqing Gao, Jasmine Annie Wu for their assistance in literature survey and helpful discussions.

REFERENCES

(1) Qiu, Z.; Hammer, B. A. G.; Müllen, K. Conjugated polymers—Problems and promises. *Prog. Polym. Sci.* **2020**, *100*, 101179.

(2) Inal, S.; Rivnay, J.; Suiu, A.-O.; Malliaras, G. G.; McCulloch, I. Conjugated Polymers in Bioelectronics. *Acc. Chem. Res.* **2018**, *51* (6), 1368−1376.

(3) Heeger, A. J. Nobel Lecture: Semiconducting and metallic polymers: The fourth generation of polymeric materials. *Rev. Mod. Phys.* **2001**, *73* (3), 681−700.

(4) Yoon, S.; Park, S.; Park, S. H.; Nah, S.; Lee, S.; Lee, J.-W.; Ahn, H.; Yu, H.; Shin, E.-Y.; Kim, B. J.; et al. High-performance scalable organic photovoltaics with high thickness tolerance from 1 cm^2 to above 50 cm^2. *Joule* **2022**, *6* (10), 2406−2422.

(5) Zhao, X.; Zhan, X. Electron transporting semiconducting polymers in organic electronics. *Chem. Soc. Rev.* **2011**, *40* (7), 3728−3743.

(6) Zhang, G.; Zhao, J.; Chow, P. C. Y.; Jiang, K.; Zhang, J.; Zhu, Z.; Zhang, J.; Huang, F.; Yan, H. Nonfullerene Acceptor Molecules for Bulk Heterojunction Organic Solar Cells. *Chem. Rev.* **2018**, *118* (7), 3447−3507.

(7) Zhao, Y.; Guo, Y.; Liu, Y. 25th Anniversary Article: Recent Advances in n-Type and Ambipolar Organic Field-Effect Transistors. *Adv. Mater.* **2013**, *25* (38), 5372−5391.

(8) Yang, J.; Zhao, Z.; Wang, S.; Guo, Y.; Liu, Y. Insight into High-Performance Conjugated Polymers for Organic Field-Effect Transistors. *Chem* **2018**, *4* (12), 2748−2785.

(9) Jia, H.; Lei, T. Emerging research directions for n-type conjugated polymers. *J. Mater. Chem. C* **2019**, *7* (41), 12809−12821.

(10) Gross, M.; Müller, D. C.; Nothofer, H.-G.; Scherf, U.; Neher, D.; Bräuchle, C.; Meerholz, K. Improving the performance of doped π-conjugated polymers for use in organic light-emitting diodes. *Nature* **2000**, *405* (6787), 661−665.

(11) Sekine, C.; Tsubata, Y.; Yamada, T.; Kitano, M.; Doi, S. Recent progress of high performance polymer OLED and OPV materials for organic printed electronics. *Sci. Technol. Adv. Mater.* **2014**, *15* (3), 034203.

(12) Deng, X.-Y.; Zhang, Z.; Lei, T. Integrated Materials Design and Process Engineering for n-Type Polymer Thermoelectrics. *JACS Au* **2024**, *4* (11), 4066−4083.

(13) Li, P.; Lei, T. Molecular design strategies for high-performance organic electrochemical transistors. *J. Polym. Sci.* **2022**, *60* (3), 377−392.
(14) Scaccabarozzi, A. D.; Basu, A.; Aniés, F.; Liu, J.; Zapata-Arteaga, O.; Warren, R.; Firdaus, Y.; Nugraha, M. I.; Lin, Y.; Campoy-Quiles, M.; et al. Doping Approaches for Organic Semiconductors. *Chem. Rev.* **2022**, *122* (4), 4420−4492.
(15) Salzmann, I.; Heimel, G.; Oehzelt, M.; Winkler, S.; Koch, N. Molecular Electrical Doping of Organic Semiconductors: Fundamental Mechanisms and Emerging Dopant Design Rules. *Acc. Chem. Res.* **2016**, *49* (3), 370−378.
(16) Coropceanu, V.; Cornil, J.; da Silva Filho, D. A.; Olivier, Y.; Silbey, R.; Brédas, J.-L. Charge Transport in Organic Semiconductors. *Chem. Rev.* **2007**, *107* (4), 926−952.
(17) Rivnay, J.; Inal, S.; Salleo, A.; Owens, R. M.; Berggren, M.; Malliaras, G. G. Organic electrochemical transistors. *Nat. Rev. Mater.* **2018**, *3* (2), 17086.
(18) Wang, S.; Zuo, G.; Kim, J.; Sirringhaus, H. Progress of Conjugated Polymers as Emerging Thermoelectric Materials. *Prog. Polym. Sci.* **2022**, *129*, 101548.
(19) Sun, Y.; Di, C.-A.; Xu, W.; Zhu, D. Advances in n-Type Organic Thermoelectric Materials and Devices. *Adv. Electron. Mater.* **2019**, *5* (11), 1800825.
(20) Kittlesen, G. P.; White, H. S.; Wrighton, M. S. Chemical derivatization of microelectrode arrays by oxidation of pyrrole and N-methylpyrrole: fabrication of molecule-based electronic devices. *J. Am. Chem. Soc.* **1984**, *106* (24), 7389−7396.
(21) Li, P.; Lei, T. Toward Ideal Biointerfacing Electronics Using Organic Electrochemical Transistors. *Acc. Mater. Res.* **2025**, *6* (7), 853−864.
(22) Ohayon, D.; Druet, V.; Inal, S. A guide for the characterization of organic electrochemical transistors and channel materials. *Chem. Soc. Rev.* **2023**, *52* (3), 1001−1023.
(23) Gao, S.; Lei, T. Neural interface devices based on organic electrochemical transistors for in-sensor memory and computing: a perspective. *Sci. Sin. Chim.* **2025**, *55* (6), 1414−1429.
(24) Pan, X.-r.; Zhang, Z.; Lei, T. Application and Prospects of Conjugated Polymers in Brain-Computer Interfaces. *Acta Polym. Sin.* **2025**, *56* (3), 377−395.
(25) Li, P.; Shi, J.; Lei, Y.; Huang, Z.; Lei, T. Switching p-type to high-performance n-type organic electrochemical transistors via doped state engineering. *Nat. Commun.* **2022**, *13* (1), 5970.
(26) Li, J.-L.; Deng, X.-Y.; Chen, J.; Fu, P.-X.; Tian, S.-Y.; Wang, Y.; Gu, X.; Lei, T. Cationic Conjugated Polymers with Enhanced Doped-State Planarity for n-Type Organic Thermoelectrics. *CCS Chem.* **2025**, *7* (5), 1449−1458.
(27) Jacobs, I. E.; Moulé, A. J. Controlling Molecular Doping in Organic Semiconductors. *Adv. Mater.* **2017**, *29* (42), 1703063.
(28) Yan, H.; Ma, W. Molecular Doping Efficiency in Organic Semiconductors: Fundamental Principle and Promotion Strategy. *Adv. Funct. Mater.* **2022**, *32* (12), 2111351.
(29) Min, J.; Kim, D.; Han, S. G.; Park, C.; Lim, H.; Sung, W.; Cho, K. Position-Induced Efficient Doping for Highly Doped Organic Thermoelectric Materials. *Adv. Electron. Mater.* **2022**, *8* (3), 2101142.
(30) Crispin, X. Thermoelectric Properties of Conducting Polymers. In *WSPC Reference on Organic Electronics: Organic Semiconductors*; World Scientific, 2016; pp 277−298.
(31) Zuo, G.; Abdalla, H.; Kemerink, M. Conjugated Polymer Blends for Organic Thermoelectrics. *Adv. Electron. Mater.* **2019**, *5* (11), 1800821.
(32) Baranovskii, S. D.; Faber, T.; Hensel, F.; Thomas, P. The applicability of the transport-energy concept to various disordered materials. *J. Phys.: Condens. Matter* **1997**, *9* (13), 2699.
(33) Li, J.; Deng, S.; Hu, J.; Liu, Y. Cation exchange improves the efficiency and stability of the n-doping of π-conjugated polymers. *J. Mater. Chem. A* **2024**, *12* (32), 21434−21441.
(34) Bubnova, O.; Khan, Z. U.; Malti, A.; Braun, S.; Fahlman, M.; Berggren, M.; Crispin, X. Optimization of the thermoelectric figure of merit in the conducting polymer poly(3,4-ethylenedioxythiophene). *Nat. Mater.* **2011**, *10* (6), 429−433.
(35) Wei, H.; Chen, P.-A.; Wu, T.; Xia, J.; Ding, J.; Zhang, Y.; Zeng, X.; Gong, Z.; Peng, C.; Xue, J.; et al. High-Miscibility n-Dopant for Organic Semiconductors Enabling Highly Stable Organic Transistors. *Adv. Funct. Mater.* **2025**, *35* (36), 2500631.
(36) Xu, C.; Wang, D. Electron transfer driving force as the criterion for efficient n-doping of organic semiconductors with DMBI-H derivatives. *J. Mater. Chem. A* **2023**, *11* (28), 15416−15425.
(37) Bernards, D. A.; Malliaras, G. G. Steady-State and Transient Behavior of Organic Electrochemical Transistors. *Adv. Funct. Mater.* **2007**, *17* (17), 3538−3544.
(38) Inal, S.; Malliaras, G. G.; Rivnay, J. Benchmarking organic mixed conductors for transistors. *Nat. Commun.* **2017**, *8* (1), 1767.
(39) Keene, S. T.; Laulainen, J. E. M.; Pandya, R.; Moser, M.; Schnedermann, C.; Midgley, P. A.; McCulloch, I.; Rao, A.; Malliaras, G. G. Hole-limited electrochemical doping in conjugated polymers. *Nat. Mater.* **2023**, *22* (9), 1121−1127.
(40) Yuen, J. D.; Dhoot, A. S.; Namdas, E. B.; Coates, N. E.; Heeney, M.; McCulloch, I.; Moses, D.; Heeger, A. J. Electrochemical Doping in Electrolyte-Gated Polymer Transistors. *J. Am. Chem. Soc.* **2007**, *129* (46), 14367−14371.
(41) Shimotani, H.; Diguet, G.; Iwasa, Y. Direct comparison of field-effect and electrochemical doping in regioregular poly(3-hexylthiophene). *Appl. Phys. Lett.* **2005**, *86* (2), 022104.
(42) Guo, J.; Xu, K.; Asatryan, J.; Alonso-Navarro, M. J.; Zapata-Arteaga, O.; Craighero, M.; Perevedentsev, A.; Kroon, R.; Mar Ramos, M.; Segura, J. L.; et al. Microstructural Evolution Dominates the Changes in the Thermal Conductivity of Conjugated Polymers Upon Doping. *Adv. Funct. Mater.* **2025**, No. e10822.
(43) Siemons, N.; Pearce, D.; Cendra, C.; Yu, H.; Tuladhar, S. M.; Hallani, R. K.; Sheelamanthula, R.; LeCroy, G. S.; Siemons, L.; White, A. J. P.; et al. Impact of Side-Chain Hydrophilicity on Packing, Swelling, and Ion Interactions in Oxy-Bithiophene Semiconductors. *Adv. Mater.* **2022**, *34* (39), 2204258.
(44) Xiao, M.; Carey, R. L.; Chen, H.; Jiao, X.; Lemaur, V.; Schott, S.; Nikolka, M.; Jellett, C.; Sadhanala, A.; Rogers, S.; et al. Charge transport physics of a unique class of rigid-rod conjugated polymers with fused-ring conjugated units linked by double carbon-carbon bonds. *Sci. Adv.* **2021**, *7* (18), No. eabe5280.
(45) Voss, M. G.; Challa, J. R.; Scholes, D. T.; Yee, P. Y.; Wu, E. C.; Liu, X.; Park, S. J.; León Ruiz, O.; Subramaniyan, S.; Chen, M.; et al. Driving Force and Optical Signatures of Bipolaron Formation in Chemically Doped Conjugated Polymers. *Adv. Mater.* **2021**, *33* (3), 2000228.
(46) Aubry, T. J.; Winchell, K. J.; Salamat, C. Z.; Basile, V. M.; Lindemuth, J. R.; Stauber, J. M.; Axtell, J. C.; Kubena, R. M.; Phan, M. D.; Bird, M. J.; et al. Tunable Dopants with Intrinsic Counterion Separation Reveal the Effects of Electron Affinity on Dopant Intercalation and Free Carrier Production in Sequentially Doped Conjugated Polymer Films. *Adv. Funct. Mater.* **2020**, *30* (28), 2001800.
(47) Duong, D. T.; Wang, C.; Antono, E.; Toney, M. F.; Salleo, A. The chemical and structural origin of efficient p-type doping in P3HT. *Org. Electron.* **2013**, *14* (5), 1330−1336.
(48) Kroon, R.; Kiefer, D.; Stegerer, D.; Yu, L.; Sommer, M.; Müller, C. Polar Side Chains Enhance Processability, Electrical Conductivity, and Thermal Stability of a Molecularly p-Doped Polythiophene. *Adv. Mater.* **2017**, *29* (24), 1700930.
(49) Moser, M.; Gladisch, J.; Ghosh, S.; Hidalgo, T. C.; Ponder, J. F., Jr.; Sheelamanthula, R.; Thiburce, Q.; Gasparini, N.; Wadsworth, A.; Salleo, A.; et al. Controlling Electrochemically Induced Volume Changes in Conjugated Polymers by Chemical Design: from Theory to Devices. *Adv. Funct. Mater.* **2021**, *31* (26), 2100723.
(50) Nicolini, T.; Surgailis, J.; Savva, A.; Scaccabarozzi, A. D.; Nakar, R.; Thuau, D.; Wantz, G.; Richter, L. J.; Dautel, O.; Hadziioannou, G.; et al. A Low-Swelling Polymeric Mixed Conductor Operating in Aqueous Electrolytes. *Adv. Mater.* **2021**, *33* (2), 2005723.

(51) Tsarfati, Y.; Bustillo, K. C.; Savitzky, B. H.; Balhorn, L.; Quill, T. J.; Marks, A.; Donohue, J.; Zeltmann, S. E.; Takacs, C. J.; Giovannitti, A.; et al. The hierarchical structure of organic mixed ionic−electronic conductors and its evolution in water. *Nat. Mater.* **2025**, *24* (1), 101−108.
(52) Wu, Y.; Zhao, Y.; Liu, Y. Toward Efficient Charge Transport of Polymer-Based Organic Field-Effect Transistors: Molecular Design, Processing, and Functional Utilization. *Acc. Mater. Res.* **2021**, *2* (11), 1047−1058.
(53) Che, Y.; Perepichka, D. F. Quantifying Planarity in the Design of Organic Electronic Materials. *Angew. Chem., Int. Ed.* **2021**, *60* (3), 1364−1373.
(54) Zhou, Y.; Zhang, K.; Chen, Z.; Zhang, H. Molecular Design Concept for Enhancement Charge Carrier Mobility in OFETs: A Review. *Materials* **2023**, *16* (20), 6645.
(55) Yan, X.; Xiong, M.; Deng, X.-Y.; Liu, K.-K.; Li, J.-T.; Wang, X.-Q.; Zhang, S.; Prine, N.; Zhang, Z.; Huang, W.; et al. Approaching disorder-tolerant semiconducting polymers. *Nat. Commun.* **2021**, *12* (1), 5723.
(56) Ding, J.; Liu, Z.; Zhao, W.; Jin, W.; Xiang, L.; Wang, Z.; Zeng, Y.; Zou, Y.; Zhang, F.; Yi, Y.; et al. Selenium-Substituted Diketopyrrolopyrrole Polymer for High-Performance p-Type Organic Thermoelectric Materials. *Angew. Chem., Int. Ed.* **2019**, *58* (52), 18994−18999.
(57) Huang, Z.; Li, P.; Lei, Y.; Deng, X.-Y.; Chen, Y.-N.; Tian, S.; Pan, X.; Lei, X.; Song, C.; Zheng, Y.; et al. Azonia-Naphthalene: A Cationic Hydrophilic Building Block for Stable N-Type Organic Mixed Ionic-Electronic Conductors. *Angew. Chem., Int. Ed.* **2024**, *63* (6), No. e202313260.
(58) Ge, G.-Y.; Xu, J.; Wang, X.; Sun, W.; Yang, M.; Mei, Z.; Deng, X.-Y.; Li, P.; Pan, X.; Li, J.-T.; et al. On-site biosignal amplification using a single high-spin conjugated polymer. *Nat. Commun.* **2025**, *16* (1), 396.
(59) Qi, G.; Wang, M.; Wang, S.; Zhang, S.; Teng, X.; Bai, H.; Wang, B.; Zhao, C.; Su, W.; Fan, Q.; et al. High-Performance, Single-Component Ambipolar Organic Electrochemical Transistors with Balanced n/p-Type Properties for Inverter and Biosensor Applications. *Adv. Funct. Mater.* **2025**, *35* (2), 2413112.
(60) Chen, Z.; Ding, X.; Wang, J.; Guo, X.; Shao, S.; Feng, K. π-Conjugated Polymers for High-Performance Organic Electrochemical Transistors: Molecular Design Strategies, Applications and Perspectives. *Angew. Chem., Int. Ed.* **2025**, *64* (7), No. e202423013.
(61) Moser, M.; Savva, A.; Thorley, K.; Paulsen, B. D.; Hidalgo, T. C.; Ohayon, D.; Chen, H.; Giovannitti, A.; Marks, A.; Gasparini, N.; et al. Polaron Delocalization in Donor−Acceptor Polymers and its Impact on Organic Electrochemical Transistor Performance. *Angew. Chem., Int. Ed.* **2021**, *60* (14), 7777−7785.
(62) Shi, Y.; Li, J.; Sun, H.; Li, Y.; Wang, Y.; Wu, Z.; Jeong, S. Y.; Woo, H. Y.; Fabiano, S.; Guo, X. Thiazole Imide-Based All-Acceptor Homopolymer with Branched Ethylene Glycol Side Chains for Organic Thermoelectrics. *Angew. Chem., Int. Ed.* **2022**, *61* (51), No. e202214192.
(63) Shi, L.; Yang, H.; Li, H.; Kuang, Y.; Ma, M.; Shao, S.; Xie, Z.; Liu, J. Controlling ambipolar OECT threshold voltage through acceptor unit engineering of conjugated polymers. *J. Mater. Chem. C* **2025**, *13* (37), 19437−19443.
(64) Wang, J.; Wu, C.; Ren, Z.; Tian, S.-Y.; Ding, Q.; Pan, X.; Deng, X.-Y.; Chen, J.; Li, J.; Wang, J.; et al. Achieving Ultrahigh n-Type Thermoelectric Power Factor in an Intrinsically Large Transport-Fermi Energy Gap Conjugated Polymer. *Adv. Mater.* **2025**, No. e12453.
(65) Gao, Y.; Ke, Y.; Wang, T.; Shi, Y.; Wang, C.; Ding, S.; Wang, Y.; Deng, Y.; Hu, W.; Geng, Y. An n-Type Conjugated Polymer with Low Crystallinity for High-Performance Organic Thermoelectrics. *Angew. Chem., Int. Ed.* **2024**, *63* (20), No. e202402642.
(66) Pan, X.; Ren, Z.; Chen, Y.; Zheng, Y.; Li, P.; Sun, W.; Xu, J.; Chen, J.-P.; Ge, G.-Y.; Li, Q.; et al. Strong Proquinoidal Acceptor Enables High-Performance Ambipolar Organic Electrochemical Transistors. *Adv. Mater.* **2025**, *37* (15), 2417146.
(67) Lv, S.; Li, L.; Mu, Y.; Wan, X. Side-chain engineering as a powerful tool to tune the properties of polymeric field-effect transistors. *Polym. Rev.* **2021**, *61* (3), 520−552.
(68) Jia, H.; Huang, Z.; Li, P.; Zhang, S.; Wang, Y.; Wang, J.-Y.; Gu, X.; Lei, T. Engineering donor−acceptor conjugated polymers for high-performance and fast-response organic electrochemical transistors. *J. Mater. Chem. C* **2021**, *9* (14), 4927−4934.
(69) Flagg, L. Q.; Bischak, C. G.; Onorato, J. W.; Rashid, R. B.; Luscombe, C. K.; Ginger, D. S. Polymer Crystallinity Controls Water Uptake in Glycol Side-Chain Polymer Organic Electrochemical Transistors. *J. Am. Chem. Soc.* **2019**, *141* (10), 4345−4354.
(70) Bardagot, O.; DiTullio, B. T.; Jones, A. L.; Speregen, J.; Reynolds, J. R.; Banerji, N. Balancing Electroactive Backbone and Oligo(Ethylene Oxy) Side-Chain Content Improves Stability and Performance of Soluble PEDOT Copolymers in Organic Electrochemical Transistors. *Adv. Funct. Mater.* **2025**, *35* (7), 2412554.
(71) Yu, Z.; Jiang, X.; Shi, C.; Shi, Y.; Huang, L.; Han, Y.; Deng, Y.; Geng, Y. Anisole Processible n-Type Conjugated Polymers Synthesized via C−H/C−H Oxidative Direct Arylation Polycondensation for Organic Electrochemical Transistors. *Macromol. Rapid Commun.* **2025**, *46* (4), 2400757.
(72) Tanaka, H.; Kanahashi, K.; Takekoshi, N.; Mada, H.; Ito, H.; Shimoi, Y.; Ohta, H.; Takenobu, T. Thermoelectric properties of a semicrystalline polymer doped beyond the insulator-to-metal transition by electrolyte gating. *Sci. Adv.* **2020**, *6* (7), No. eaay8065.
(73) Ma, M.; Zhang, L.; Huang, M.; Kuang, Y.; Li, H.; Yang, H.; Yao, T.; Ye, G.; Shao, S.; Yoon, M.-H.; et al. Regiochemistry and Side-Chain Engineering Enable Efficient N-Type Mixed Conducting Polymers. *Angew. Chem., Int. Ed.* **2025**, *64* (21), No. e202424820.
(74) Liu, J.; Qiu, L.; Alessandri, R.; Qiu, X.; Portale, G.; Dong, J.; Talsma, W.; Ye, G.; Sengrian, A. A.; Souza, P. C. T.; et al. Enhancing Molecular n-Type Doping of Donor−Acceptor Copolymers by Tailoring Side Chains. *Adv. Mater.* **2018**, *30* (7), 1704630.
(75) Liu, J.; Ye, G.; Potgieser, H. G. O.; Koopmans, M.; Sami, S.; Nugraha, M. I.; Villalva, D. R.; Sun, H.; Dong, J.; Yang, X.; et al. Amphipathic Side Chain of a Conjugated Polymer Optimizes Dopant Location toward Efficient N-Type Organic Thermoelectrics. *Adv. Mater.* **2021**, *33* (4), 2006694.
(76) Song, Y.; Ding, J.; Dai, X.; Li, C.; Di, C.-a.; Zhang, D. Enhancement of the Thermoelectric Performance of n-Type Naphthalene Diimide-Based Conjugated Polymer by Engineering of Side Alkyl Chains. *ACS Mater. Lett.* **2022**, *4* (4), 521−527.
(77) Ma, M.; Ye, G.; Jang, S.; Kuang, Y.; Zhang, L.; Shao, S.; Koster, L. J. A.; Baran, D.; Liu, J. Realizing an N-Type Organic Thermoelectric ZT of 0.46. *ACS Energy Lett.* **2025**, *10* (4), 1813−1820.
(78) Ye, G.; Kuang, Y.; Ma, M.; Peng, X.; Liu, J. Fluorinated Alkyl Chains Terminated Polar Glycol Ether Side Chain for N-Type Organic Thermoelectrics with Enhanced Performance and Air Stability. *Adv. Sci.* **2025**, *12* (25), 2500571.
(79) Shi, H.; Liu, C.; Jiang, Q.; Xu, J. Effective Approaches to Improve the Electrical Conductivity of PEDOT:PSS: A Review. *Adv. Electron. Mater.* **2015**, *1* (4), 1500017.
(80) Heywang, G.; Jonas, F. Poly(alkylenedioxythiophene)s—new, very stable conducting polymers. *Adv. Mater.* **1992**, *4* (2), 116−118.
(81) Sato, K.; Yamaura, M.; Hagiwara, T.; Murata, K.; Tokumoto, M. Study on the electrical conduction mechanism of polypyrrole films. *Synth. Met.* **1991**, *40* (1), 35−48.
(82) Wang, S.; Sun, H.; Ail, U.; Vagin, M.; Persson, P. O. Å.; Andreasen, J. W.; Thiel, W.; Berggren, M.; Crispin, X.; Fazzi, D.; et al. Thermoelectric Properties of Solution-Processed n-Doped Ladder-Type Conducting Polymers. *Adv. Mater.* **2016**, *28* (48), 10764−10771.
(83) Guo, J.; Flagg, L. Q.; Tran, D. K.; Chen, S. E.; Li, R.; Kolhe, N. B.; Giridharagopal, R.; Jenekhe, S. A.; Richter, L. J.; Ginger, D. S. Hydration of a Side-Chain-Free n-Type Semiconducting Ladder Polymer Driven by Electrochemical Doping. *J. Am. Chem. Soc.* **2023**, *145* (3), 1866−1876.

(84) Wang, X.; Jiang, H.; Wang, H.; Chen, W.; Wang, R.; Zhong, Y.; Tang, Z.; Chen, Z.; Li, H.; Duan, X.; et al. Shear-Intensified Hybridization of Conjugated Polymer Fibers for Organic Electrochemical Transistors. *Adv. Funct. Mater.* **2025**, No. e15197.
(85) Kim, N.; Kee, S.; Lee, S. H.; Lee, B. H.; Kahng, Y. H.; Jo, Y.-R.; Kim, B.-J.; Lee, K. Highly Conductive PEDOT:PSS Nanofibrils Induced by Solution-Processed Crystallization. *Adv. Mater.* **2014**, *26* (14), 2268−2272.
(86) Cheung, K. M.; Bloor, D.; Stevens, G. C. The influence of unusual counterions on the electrochemistry and physical properties of polypyrrole. *J. Mater. Sci.* **1990**, *25* (9), 3814−3837.
(87) Culebras, M.; Gómez, C. M.; Cantarero, A. Enhanced thermoelectric performance of PEDOT with different counter-ions optimized by chemical reduction. *J. Mater. Chem. A* **2014**, *2* (26), 10109−10115.
(88) Li, P.; Sun, W.; Li, J.; Chen, J.-P.; Wang, X.; Mei, Z.; Jin, G.; Lei, Y.; Xin, R.; Yang, M.; et al. N-type semiconducting hydrogel. *Science* **2024**, *384* (6695), 557−563.
(89) Qiu, L.; Liu, J.; Alessandri, R.; Qiu, X.; Koopmans, M.; Havenith, R. A.; Marrink, S. J.; Chiechi, R. C.; Anton Koster, L. J.; Hummelen, J. C. Enhancing doping efficiency by improving host-dopant miscibility for fullerene-based n-type thermoelectrics. *J. Mater. Chem. A* **2017**, *5* (40), 21234−21241.
(90) Lin, X.; Wegner, B.; Lee, K. M.; Fusella, M. A.; Zhang, F.; Moudgil, K.; Rand, B. P.; Barlow, S.; Marder, S. R.; Koch, N.; et al. Beating the thermodynamic limit with photo-activation of n-doping in organic semiconductors. *Nat. Mater.* **2017**, *16* (12), 1209−1215.
(91) Guo, H.; Yang, C.-Y.; Zhang, X.; Motta, A.; Feng, K.; Xia, Y.; Shi, Y.; Wu, Z.; Yang, K.; Chen, J.; et al. Transition metal-catalysed molecular n-doping of organic semiconductors. *Nature* **2021**, *599* (7883), 67−73.
(92) Wang, X.-Y.; Ding, Y.-F.; Zhang, X.-Y.; Zhou, Y.-Y.; Pan, C.-K.; Li, Y.-H.; Liu, N.-F.; Yao, Z.-F.; Chen, Y.-S.; Xie, Z.-H.; et al. Light-triggered regionally controlled n-doping of organic semiconductors. *Nature* **2025**, *642* (8068), 599−604.
(93) Wu, C.; Lei, T. From Light to Logic: Micron-Scale Doping Enables Flexible Organic Circuits. *Polym. Sci. Technol.* **2025**, *1* (6), 500−502.
(94) Jacobs, I. E.; Lin, Y.; Huang, Y.; Ren, X.; Simatos, D.; Chen, C.; Tjhe, D.; Statz, M.; Lai, L.; Finn, P. A.; et al. High-Efficiency Ion-Exchange Doping of Conducting Polymers. *Adv. Mater.* **2022**, *34* (22), 2102988.
(95) Xiong, M.; Deng, X.-Y.; Tian, S.-Y.; Liu, K.-K.; Fang, Y.-H.; Wang, J.-R.; Wang, Y.; Liu, G.; Chen, J.; Villalva, D. R.; et al. Counterion docking: a general approach to reducing energetic disorder in doped polymeric semiconductors. *Nat. Commun.* **2024**, *15* (1), 4972.
(96) Ishii, M.; Yamashita, Y.; Watanabe, S.; Ariga, K.; Takeya, J. Doping of molecular semiconductors through proton-coupled electron transfer. *Nature* **2023**, *622* (7982), 285−291.
(97) Rudd, S.; Franco-Gonzalez, J. F.; Kumar Singh, S.; Ullah Khan, Z.; Crispin, X.; Andreasen, J. W.; Zozoulenko, I.; Evans, D. Charge transport and structure in semimetallic polymers. *J. Polym. Sci., Polym. Phys.* **2018**, *56* (1), 97−104.
(98) Wang, D.; Ding, J.; Dai, X.; Xiang, L.; Ye, D.; He, Z.; Zhang, F.; Jung, S.-H.; Lee, J.-K.; Di, C.-a.; et al. Triggering ZT to 0.40 by Engineering Orientation in One Polymeric Semiconductor. *Adv. Mater.* **2023**, *35* (2), 2208215.
(99) Liu, K.; Wang, J.; Pan, X.; Tian, S.-Y.; Liu, Y.; Zhang, Z.; Di, Y.; Chen, J.; Wu, C.; Deng, X.-Y.; et al. n-Type thermoelectric elastomers. *Nature* **2025**, *644* (8078), 920−926.
(100) Wang, X.-Y.; Yu, Z.-D.; Lu, Y.; Yao, Z.-F.; Zhou, Y.-Y.; Pan, C.-K.; Liu, Y.; Wang, Z.-Y.; Ding, Y.-F.; Wang, J.-Y.; et al. Density of States Engineering of n-Doped Conjugated Polymers for High Charge Transport Performances. *Adv. Mater.* **2023**, *35* (21), 2300634.
(101) Deng, S.; Kuang, Y.; Liu, L.; Liu, X.; Liu, J.; Li, J.; Meng, B.; Di, C.-a.; Hu, J.; Liu, J. High-Performance and Ecofriendly Organic Thermoelectrics Enabled by N-Type Polythiophene Derivatives with Doping-Induced Molecular Order. *Adv. Mater.* **2024**, *36* (8), 2309679.
(102) Xiong, M.; Yan, X.; Li, J.-T.; Zhang, S.; Cao, Z.; Prine, N.; Lu, Y.; Wang, J.-Y.; Gu, X.; Lei, T. Efficient n-Doping of Polymeric Semiconductors through Controlling the Dynamics of Solution-State Polymer Aggregates. *Angew. Chem., Int. Ed.* **2021**, *60* (15), 8189−8197.
(103) Zhang, Z.; Li, P.; Xiong, M.; Zhang, L.; Chen, J.; Lei, X.; Pan, X.; Wang, X.; Deng, X.-Y.; Shen, W.; et al. Continuous production of ultratough semiconducting polymer fibers with high electronic performance. *Sci. Adv.* **2024**, *10* (14), No. eadk0647.
(104) Wang, D.; Ding, J.; Ma, Y.; Xu, C.; Li, Z.; Zhang, X.; Zhao, Y.; Zhao, Y.; Di, Y.; Liu, L.; et al. Multi-heterojunctioned plastics with high thermoelectric figure of merit. *Nature* **2024**, *632* (8025), 528−535.
(105) Moser, M.; Hidalgo, T. C.; Surgailis, J.; Gladisch, J.; Ghosh, S.; Sheelamanthula, R.; Thiburce, Q.; Giovannitti, A.; Salleo, A.; Gasparini, N.; et al. Side Chain Redistribution as a Strategy to Boost Organic Electrochemical Transistor Performance and Stability. *Adv. Mater.* **2020**, *32* (37), 2002748.
(106) Uguz, I.; Ohayon, D.; Yilmaz, S.; Griggs, S.; Sheelamanthula, R.; Fabbri, J. D.; McCulloch, I.; Inal, S.; Shepard, K. L. Complementary integration of organic electrochemical transistors for front-end amplifier circuits of flexible neural implants. *Sci. Adv.* **2024**, *10* (12), No. eadi9710.
(107) Zhu, M.; Li, P.; Li, J.-L.; Lei, T. Molecular packing and film morphology control in organic electrochemical transistors. *Mol. Syst. Des. Eng.* **2022**, *7* (1), 6−20.
(108) Huang, L.; Wang, Z.; Chen, J.; Wang, B.; Chen, Y.; Huang, W.; Chi, L.; Marks, T. J.; Facchetti, A. Porous Semiconducting Polymers Enable High-Performance Electrochemical Transistors. *Adv. Mater.* **2021**, *33* (14), 2007041.
(109) Wang, X.; Zhang, Z.; Li, P.; Xu, J.; Zheng, Y.; Sun, W.; Xie, M.; Wang, J.; Pan, X.; Lei, X.; et al. Ultrastable N-Type Semiconducting Fiber Organic Electrochemical Transistors for Highly Sensitive Biosensors. *Adv. Mater.* **2024**, *36* (24), 2400287.
(110) Tan, S. T. M.; Lee, G.; Denti, I.; LeCroy, G.; Rozylowicz, K.; Marks, A.; Griggs, S.; McCulloch, I.; Giovannitti, A.; Salleo, A. Tuning Organic Electrochemical Transistor Threshold Voltage using Chemically Doped Polymer Gates. *Adv. Mater.* **2022**, *34* (33), 2202359.
(111) Spyropoulos, G. D.; Gelinas, J. N.; Khodagholy, D. Internal ion-gated organic electrochemical transistor: A building block for integrated bioelectronics. *Sci. Adv.* **2019**, *5* (2), No. eaau7378.
(112) Yan, C.; Xiang, L.; Xiao, Y.; Zhang, X.; Jiang, Z.; Zhang, B.; Li, C.; Di, S.; Zhang, F. Lateral intercalation-assisted ionic transport towards high-performance organic electrochemical transistor. *Nat. Commun.* **2024**, *15* (1), 10118.
(113) Flagg, L. Q.; Bischak, C. G.; Quezada, R. J.; Onorato, J. W.; Luscombe, C. K.; Ginger, D. S. P-Type Electrochemical Doping Can Occur by Cation Expulsion in a High-Performing Polymer for Organic Electrochemical Transistors. *ACS Mater. Lett.* **2020**, *2* (3), 254−260.
(114) Kukhta, N. A.; Marks, A.; Luscombe, C. K. Molecular Design Strategies toward Improvement of Charge Injection and Ionic Conduction in Organic Mixed Ionic−Electronic Conductors for Organic Electrochemical Transistors. *Chem. Rev.* **2022**, *122* (4), 4325−4355.
(115) Lingstedt, L. V.; Ghittorelli, M.; Lu, H.; Koutsouras, D. A.; Marszalek, T.; Torricelli, F.; Crăciun, N. I.; Gkoupidenis, P.; Blom, P. W. M. Effect of DMSO Solvent Treatments on the Performance of PEDOT:PSS Based Organic Electrochemical Transistors. *Adv. Electron. Mater.* **2019**, *5* (3), 1800804.
(116) Rivnay, J.; Leleux, P.; Ferro, M.; Sessolo, M.; Williamson, A.; Koutsouras, D. A.; Khodagholy, D.; Ramuz, M.; Strakosas, X.; Owens, R. M.; et al. High-performance transistors for bioelectronics through tuning of channel thickness. *Sci. Adv.* **2015**, *1* (4), No. e1400251.
(117) Wu, R.; Meli, D.; Strzalka, J.; Narayanan, S.; Zhang, Q.; Paulsen, B. D.; Rivnay, J.; Takacs, C. J. Bridging length scales in

organic mixed ionic−electronic conductors through internal strain and mesoscale dynamics. *Nat. Mater.* **2024**, *23* (5), 648−655.
(118) Russ, B.; Glaudell, A.; Urban, J. J.; Chabinyc, M. L.; Segalman, R. A. Organic thermoelectric materials for energy harvesting and temperature control. *Nat. Rev. Mater.* **2016**, *1* (10), 16050.
(119) LeCroy, G.; Ghosh, R.; Sommerville, P.; Burke, C.; Makki, H.; Rozylowicz, K.; Cheng, C.; Weber, M.; Khelifi, W.; Stingelin, N.; et al. Using Molecular Structure to Tune Intrachain and Interchain Charge Transport in Indacenodithiophene-Based Copolymers. *J. Am. Chem. Soc.* **2024**, *146* (31), 21778−21790.

https://doi.org/10.1021/acs.chemmater.5c02592
Chem. Mater. 2026, 38, 3−19